

國立交通大學

光電工程研究所

博士論文

鎖模摻鉕光纖雷射中的光固子現象

Soliton Phenomena in Mode-Locked Er-Fiber
Lasers



研究生：項維巍

指導教授：賴暎杰 博士

中華民國 九十五年 六月

鎖模摻鉺光纖雷射中的光固子現象

Soliton Phenomena in Mode-Locked Er-Fiber Lasers

研究生：項維巍 Student : Wei-Wei Hsiang
指導教授：賴暎杰 博士 Advisor : Dr. Yinchieh Lai

國立交通大學 電機資訊學院

光電工程研究所

博士論文



A Dissertation

Submitted in Partial Fulfillment of the Requirements
for the Degree of Doctor of Philosophy in
The Department of Photonics and
The Institute of Electro-Optical Engineering
National Chiao-Tung University
Hsinchu, Taiwan, R.O.C.

中華民國 九十五年 六月

鎖模摻鉍光纖雷射中的光固子現象

研究生：項維巍

指導教授：賴暎杰 博士

國立交通大學 電機資訊學院

光電工程研究所

摘要

本論文探討在鎖模摻鉍光纖雷射中的主要光固子現象，一方面可以利用光固子效應來實現高脈衝重複率、飛秒級的鎖模摻鉍光纖雷射，另一方面，也可以將鎖模摻鉍光纖雷射當作一個新的實驗平台，用來觀測和探討如光固子結合態之類的光固子現象。

在產生高重複率、超短脈衝序列這部分，被動諧波鎖模和非同步光固子鎖模都可以用來提高飛秒級鎖模摻鉍光纖雷射的脈衝重複率。尤其是利用非同步光固子鎖模的方式，可以從鎖模摻鉍光纖雷射直接產生重複率 10 GHz、脈寬 816 fs、超模抑制比高達 70 dB 以上的脈衝序列。而且利用非同步鎖模特有的偏移頻率之取出和鎖定，我們發展出一個簡單且經濟的方法來維持非同步鎖模雷射的長期穩定。利用此長期穩定雷射共振腔長的方法，GHz、飛秒等級的非同步鎖模摻鉍光纖雷射將具有經濟上的優勢。

在探索新的光固子現象這方面，光固子結合態可在被動或混和式頻率調變鎖模摻鉍光纖雷射中觀察到。尤其是在混和式頻率調變鎖模摻鉍光纖雷射中，我們能夠產生重複率高達 10 GHz 的新型穩定結合光固子對，並且相當於有 1177 個光固子對同時存在於雷射共振腔中。我們也已在理論上探討此光固子對的形成和穩

定機制，所獲得的結果與實驗上的觀測相當符合。



Soliton Phenomena in Mode-Locked Er-Fiber Lasers

Student: Wei-Wei Hsiang

Advisor: Dr. Yinchieh Lai

Department of Photonics and Institute of Electro-Optical Engineering
College of Electrical Engineering and Computer Science
National Chiao-Tung University

ABSTRACT

The dissertation investigates the important soliton phenomena in mode-locked Er-fiber lasers. On one hand, the soliton effects can be employed to demonstrate sub-ps mode-locked Er-fiber lasers at high repetition rates. On the other hand, the mode-locked Er-fiber lasers can be used as a handy platform for investigating new types of soliton phenomena, including the soliton bound states.

In the regard of demonstrating high-repetition-rate ultrashort pulses, passive harmonic mode-locking and asynchronous soliton mode-locking both show the ability to increase the pulse repetition rate of sub-ps mode-locked Er-fiber lasers. In particular, the 10 GHz 0.8 ps SMSR > 70 dB pulse train has been directly generated from an asynchronously mode-locked (ASM) Er-fiber soliton laser. We have also developed a simple and economic long-term stabilization method based on the deviation-frequency extraction and locking. With the scheme, sub-ps ASM Er-fiber soliton lasers with GHz repetition rates can have economic advantages for practical applications.

In the regard of demonstrating new types of soliton phenomena, the soliton bound states have been observed both in the passively mode-locked and the hybrid FM mode-locked Er-fiber lasers. Most importantly, for the first time new stable bound

soliton pairs at the 10 GHz repetition rate are observed experimentally in a hybrid FM mode-locked Er-fiber laser, in which there are 1177 soliton pairs simultaneously circulating in the laser cavity. The corresponding mechanisms for explaining the formation as well as the superior stability of these closely bound soliton pairs are theoretically investigated and experimentally examined.



致謝

在這幾年博士班生涯中，很榮幸地，能夠與許多優秀的人共事合作，讓規劃的研究工作得以進行。也很幸運地，得到了許多人的協助和鼓勵，完成了目前這些工作。

感謝指導教授賴暎杰老師帶領我成為學術研究的一份子。不論是在研究工作的討論、論文的寫作與修改、國際會議的報告等等，都給予了我極大的幫助。在此，由衷的感謝賴老師細心與耐心的教導。

感謝交大光電所祁姓教授和陳智弘教授，提供實驗上所需的儀器設備。感謝中央研究院原分所孔慶昌研究員，從我擔任研究助理到博士班畢業，總是不吝惜的給予我指導與幫助。謝謝工研院量測中心彭錦隆博士，提供了許多很有用的實驗技術。

實驗室的好朋友，澄鈴學姐、瑞光、凱評和桂珠，多虧有了你們，可以分享研究心得和生活上的點滴。

實驗室學弟妹在這論文上的功勞是不容忽視的。明哲、承知、名峰、倩仔、金水、銘峰、鐘响和人豪，不僅是非常優秀的工作伙伴，你們也增添了實驗室裡非常多的樂趣。

謝謝許多人的加油和鼓勵。張大哥，總是如此熱心地幫助我。家甄，你的話總是讓人有動力，尤其當我遇到挫折時。網球隊的小黑、Spenser，讓我的網球技術可以不要繼續退化。時雨、裴董和蔚然兄，謝謝你們在原分所的鼎力相助。朋群、偉仁、鴻章和俊庭，謝謝你們在實驗上的支援。

感謝父母和家人的支持，讓我得以專心的完成博士學業。尤其是我的母親黃豔女士，從小到大總是給我無微不至的照顧，是我永難回報的。

Contents

Chinese Abstract.....	I
English Abstract.....	III
Acknowledgements.....	V
Contents.....	VI
List of Figures.....	VIII
List of Acronyms.....	XII

Chapter 1. Introduction

1.1 Review of Mode-Locked Er-Fiber Lasers.....	1
1.2 Motivation of the Research.....	4
1.3 Organization of the Dissertation.....	5

Chapter 2. Soliton Phenomena in Passively Mode-Locked Er-Fiber Lasers

2.1 Introduction.....	11
2.2 Mater Equation, Average Soliton, and Spectral Sidebands.....	12
2.3 Saturation of APM and Soliton Energy Quantization.....	14
2.4 Passive Harmonic Mode-Locking	15
2.5 Soliton Bound States.....	19
2.6 Summary.....	20

Chapter 3. 10 GHz 0.8 ps Asynchronously Mode-Locked Er-Fiber Soliton Laser

3.1 Introduction.....	31
3.2 Asynchronous Soliton Mode-Locking.....	32
3.3 Experimental Setup.....	35

3.4	Experimental Results.....	36
3.5	Discussion and Summary.....	37

Chapter 4. Long-Term Stabilization of Asynchronously Mode-Locked Er-Fiber Soliton Laser

4.1	Introduction.....	47
4.2	Frequency Sidebands of Laser Output.....	48
4.3	Deviation-Frequency Extraction	49
4.4	Long-Term Stabilization Based on Deviation-Frequency Locking...50	
4.5	Summary.....	52

Chapter 5. New Stable 10 GHz Bound Soliton Pairs

5.1	Introduction.....	59
5.2	10 GHz Hybrid FM Mode-Locked Er-Fiber Laser.....	61
5.3	Experimental Observations of 10 GHz Bound Soliton Pairs.....	62
5.4	Theoretical Model of 10 GHz Bound Soliton Pairs.....	63
5.5	Summary.....	66

References

Chapter 6. Conclusions and Future Work

6.1	Conclusions.....	74
6.2	Future Work.....	76

References

List of Publications.....	82
----------------------------------	-----------

List of Figures

Fig. 2-1	Left: schematic diagram of the P-APM fiber laser; Right: equivalent ring cavity of the P-APM fiber laser.....	25
Fig. 2-2	Left: illustration of nonlinear rotation of elliptical polarization of P-APM; Right: the effect of saturable absorber achieved by P-APM.....	25
Fig. 2-3	Schematic diagram of experimental setup.....	26
Fig. 2-4	Optical spectra of the two different mode-locking regimes of a P-APM Er-fiber laser (a) Stretched pulse regime at fundamental repetition rate (b) Soliton regime at harmonic repetition rates.....	26
Fig. 2-5	The RF spectra when the spontaneous pulse repetition rate multiplication occurs (a) At beginning: fundamental repetition rate (b) Pulse bunching (c) Passive harmonic mode-locking.....	27
Fig. 2-6	(a) RF spectra of laser output of different harmonics M at 4, 25, and 35 respectively (b) Harmonic number versus output power.....	28
Fig. 2-7	SHG autocorrelation trace of the different soliton bound states with ps time separation (a) Two identical bound solitons (b) Five identical bound solitons with the same time separation (c) Three bound solitons with the different time separation.....	29
Fig. 2-8	Optical spectrum of the soliton bound states with ps time separation.....	30

Fig. 2-9	SHG autocorrelation trace of the bound soliton pair with fs time separation.....	30
Fig. 2-10	Optical spectrum of the bound soliton pair with fs time separation.....	30
Fig. 3-1	(a) Laser cavity with the gain, the filter, GVD, SPM and the phase modulation driven asynchronously (b) Slow modulation in asynchronous soliton mode-locking (c) Noise clean-up effect in asynchronous soliton mode-locking.....	43
Fig. 3-2	Schematic of the asynchronously mode-locked Er-fiber laser.....	44
Fig. 3-3	Optical characteristics of the pulse train from asynchronous modelocking: (a) the optical spectrum with measurement resolution=0.07nm (inset: on a linear scale).....	44
	(b) the autocorrelation trace (the solid curve) and the fitting curve (the empty circles) assuming sech^2 pulse shape.....	45
Fig. 3-4	RF spectra of the pulse train from asynchronous mode-locking:	
	(a) 20 MHz span, SMSR>70 dB.....	45
	(b) 200 kHz span, detuning frequency = 36 kHz.....	46
Fig. 4-1	RF spectra near 10 GHz. (a) Span of 50 MHz, SMSR > 70 dB	
	(b) Span of 500 kHz, deviation frequency δf of 25 kHz.....	55
Fig. 4-2	(a) Electronic frequency sidebands of laser output near DC (b) Electronics of deviation-frequency extraction (c) Electronic frequency spectrum after the lowpass filter (inset, signal in the time domain).....	56

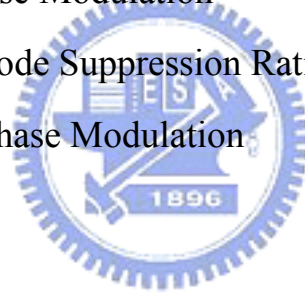
Fig. 4-3	Schematic of the mode-locked Er-fiber laser and the feedback control. BPF, band-pass filter; PD, photodiode; DSF, dispersion shift fiber.....	57
Fig. 4-4	Long-term stabilization and deviation frequency shift. Green curve: without the stabilization scheme, upper axis; blue curve: with the stabilization scheme, lower axis.....	57
Fig. 4-5	10 GHz pulse train measured from a fast sampling oscilloscope.....	58
Fig. 5-1	Bound soliton pairs in mode-locked fiber laser (a) Only one bound soliton pair circulates in the fiber laser cavity (the typical case in passively mode-locked fiber laser). (b) More than one ($N>1$) bound soliton pairs circulate simultaneously in the fiber laser cavity (the case corresponding to the 10 GHz bound soliton pairs in our hybrid FM mode-locked Er-fiber laser).....	69
Fig. 5-2	Schematic of the mode-locked Er-fiber laser and the feedback control loop. PI, proportional and integral control module; PD, photodiode.....	70
Fig. 5-3	SHG autocorrelation trace of the bound soliton pair.....	70
Fig. 5-4	Optical spectrum of the bound soliton pair (solid curve, measurement; dots, fitting).....	71
Fig. 5-5	RF spectrum of the 10 GHz bound soliton pair, SMSR > 70 dB.....	71
Fig. 5-6	Stable 10 GHz bound soliton pairs measured form the fast sampling scope.....	72

- Fig. 5-7 Timing diagram between the phase modulation signal and the bound soliton pair. M: modulation depth.....72
- Fig. 5-8 Measurements of SHG autocorrelation traces when the driving RF power of the phase modulator varies.....73
- Fig. 5-9 Time separation versus the RF power of the phase modulator (inset, timing diagram between the phase modulation signal and the bound soliton pair. M, modulation depth).....73



List of Acronyms

<u>Acronyms</u>	<u>Descriptions</u>
APM	Additive Pulse Mode-Locking
ASM	Asynchronous Mode-Locking
FM	Frequency Modulation
GVD	Group Velocity Dispersion
P-APM	Polarization Additive Pulse Mode-Locking
PZT	Piezoelectric Translator
SAM	Self Amplitude Modulation
SESAMs	SEmiconductor Saturable Absorber Mirrors
SPM	Self Phase Modulation
SMSR	Supermode Suppression Ratio
XPM	Cross Phase Modulation



Chapter 1

Introduction

1.1 Review of Mode-Locked Er-Fiber Lasers

Mode-locked fiber lasers have been developed over the past decades and they have shown the abilities to meet the specific requirements for various applications ranging from ultrafast science researches to optical telecommunication industrial technologies [1-11]. Nowadays a lot of efforts are still being devoted to implement new mode-locked fiber lasers along the directions of generating shorter pulse width and/or more-energetic pulses at higher repetition rates [12-15]. Due to the advantages of low cost, compact volume, reliable turnkey operation and long-term stabilization, mode-locked fiber lasers offer attractive alternatives of ultrashort pulse laser sources when compared to the expensive and bulky solid state mode-locked lasers [16].

Although most of the early works on fiber lasers focused on Nd-doped fiber laser [17], the 1.5 μm Er-doped fiber lasers started to receive a lot of attention due to their potential for the applications in optical fiber communication. This is because the gain spectrum of erbium-doped fiber just falls within the lower loss window of silica glass fiber. The success in the development of mode-locked Er-fiber lasers can be attributed to the following important aspects: the realization of erbium-doped fiber amplifier (EDFA) with efficient diode pumping [18], the invention of artificial fast saturable absorber based on polarization additive pulse mode-locking (P-APM) [19-21], the ability to tailor the sign and value of group dispersion velocity (GVD) of single mode fibers in the wavelength around 1.55 μm , and the implementation of all-fiber passive and active optical devices.

As the same as other mode-locked lasers, Er-fiber lasers can be mode-locked actively or passively. The two different mode-locking mechanisms result in quite different characteristics of laser output pulses [1]. Passively mode-locked Er-fiber lasers have been used to generate ultrashort pulses as short as 77 fs [22], and actively mode-locked Er-fiber lasers have been used to increase the repetition rate up to 40 GHz or higher [9].

In passively mode-locked Er-fiber lasers, saturable absorber action is required for pulse formation and pulse shortening. In the 1990s, the polarization additive pulse mode-locking (P-APM) techniques were successfully developed to replace the real saturable absorbers, such as the semiconductor saturable absorber mirrors (SESAMs) [23,24], in the fiber laser cavity. In fiber lasers, the additive pulse mode-locking (APM) is typically achieved by using only a single laser cavity. The two polarization lights propagating in the same fiber ring cavity will experience different phase shifts due to the Kerr nonlinearity of optical fibers. Therefore with a suitable initial phase bias, the nonlinear interference between these two polarization lights after a length of optical fiber can lead to intensity-dependent nonlinear polarization rotation (NPM) [25]. By using a polarizer and the effects of NPR, the intensity dependent loss, i.e., artificial saturable absorber, can be implemented. Because of the response time of Kerr nonlinearity is faster than the recovery time of SESAMs, the shortest pulse width in the 1.5 μm band is achieved by using the P-APM Er-fiber laser. In the design of ultrashort fiber lasers, besides the mode-locking mechanism of P-APM, the group velocity dispersion (GVD) and the self phase modulation (SPM) are also two other important effects which determine the achievable pulse width. It is well known that solitons can form in the optical fiber because of the co-effects of GVD and SPM. The solitary solutions also can be found from the master equation of mode-locking, where the terms of self amplitude modulation (SAM), gain dispersion, GVD and SPM are all

included [24]. Experimentally, all-fiber P-APM lasers have shown to be able to generate femtosecond soliton pulses and can selfstart to mode-locking. However, for the generation of the shortest femtosecond pulse in P-APM Er-fiber lasers, it may be advantageous to operate in the stretched pulse regime instead of the soliton regime [22]. The saturation of P-APM and the resonance of spectrum sidebands in the soliton regime limit the achievable minimum pulse width in the soliton regime [26].

P-APM Er-fiber lasers offer another advantage: all-fiber configuration. This is because the effects of NPR and polarization controllers can be implemented by a length of optical fiber utilizing the properties of fiber nonlinearity and birefringence. However, the requirement of enough nonlinear phase shift in P-APM Er-fiber lasers needs both long lengths of single mode fiber and erbium-doped fiber. This makes it very difficult to achieve a femtosecond P-APM fiber laser at a repetition rate higher than 200 MHz.

Actively mode-locked Er-fiber lasers have been demonstrated to be able to generate pulse trains in the $1.5\text{-}\mu\text{m}$ regime with a very high repetition rate. By using the technique of active harmonic mode-locking, the repetition rate up to 40 GHz or even higher can be achieved. However, there are still some more issues needed to be dealt with for actively mode-locked Er-fiber lasers. These include the issues for supermode noise, long-term stabilization, and long pulse-width. The supermode noise can be suppressed effectively by using the techniques of intracavity Fabry-Perot filter [27], SPM with spectral filtering [28], or additive pulse limiting (APL) [8]. Long-term stabilization of fiber lasers can be achieved by pulse phase locking [29] or regenerative harmonic mode-locking [9]. However, the pulse-width of actively mode-locked fiber lasers are typically in the picosecond range when the modulation frequency is less than 40 GHz. Up to now, direct generation of GHz femtosecond pulses from a mode-locked fiber laser is still very challenging, because the passive

and active mode-locking techniques are typically not combined very well in a mode-locked fiber laser.

1.2 Motivation of the Research

The ultimate goal of this research is to provide a scheme to implement a high-power, ultrashort, high-repetition-rate, all-fiber pulsed light source [30], which can be used in practical applications, like high-speed fiber communication, GHz supercontinuum generation, ultrafast optical signal processing, and quantum optics experiments such as squeezed state generation. This goal can be achieved step-by-step by utilizing the configuration of master oscillator power amplifier (MOPA). One can firstly build a high-repetition-rate femtosecond pulsed light source and then use a high power fiber amplifier to boost the pulse energy. Recently, the rapid progress in the fabrication of special fibers, such as Er/Yb codoped double-cladding fibers or large mode area fibers have made it possible to demonstrate a high-power pulsed fiber amplifier [31]. However, the master oscillator for GHz femtosecond pulses is still not accessible by using typical mode-locked fiber lasers.

The method to overcome this problem can be started from two different approaches. One can start from a femtosecond passively mode-locked fiber lasers and then try to increase the repetition rate. The other is to start from the high repetition rate actively mode-locked fiber laser and then try to shorten the pulse width. No matter which the direction one chooses to proceed, it can be found that versatile soliton effects can be utilized to achieve the required improvements mentioned above. For example, soliton energy quantization can be used to increase the repetition rate of passively mode-locked lasers [1]. The dispersive waves from the perturbed soliton have shown to be one main mechanism to evenly arrange the multiple solitons with an

equal time separation in the laser cavity. Another interesting soliton phenomenon which can be employed in the mode-locked fiber laser is the concept of sliding-frequency guiding filter, which is originally used to suppress spontaneous emission noise (ASE) in soliton communication [32,33]. The pulse experiencing continuous frequency sweep in an asynchronously mode-locked (ASM) fiber laser is analogy to the filters with the sliding center frequencies in soliton communication systems. Therefore we would like to investigate the possibility to directly generate sub-ps pulses at repetition rates more than 10 GHz from ASM fiber lasers [34].

When we are working on the development of high-repetition-rate, ultrashort mode-locked Er-fiber lasers, interesting soliton bound states have also been discovered in some occasions. These new but unknown phenomena of soliton bound states inspire us to investigate the underlying mechanisms related to soliton-soliton interaction in the mode-locked fiber lasers. Soliton bound states in passively mode-locked fiber lasers have been reported theoretically and experimentally in the literature. However, stable soliton pairs have not been observed in actively harmonic mode-locked fiber laser before. Hence it is worthwhile to investigate how more than 1000 bound soliton pairs can occur simultaneously and maintain stably in a 10 GHz hybrid FM mode-locked Er-fiber laser [35], as what we have observed in the laboratory.

1.3 Organization of the Dissertation

The dissertation is organized as follows. After the introductory part of Chapter 1, soliton phenomena in passively mode-locked Er-fiber are presented in Chapter 2. The concept of average soliton under the framework of master equation is introduced first. Then the phenomena of soliton energy quantization, spectral sidebands, passive

harmonic mode-locking, and bound soliton states are described. Chapter 3 and Chapter 4 are related to the experimental works on asynchronous soliton mode-locking. The experimental setups and results for the direct generation of 10 GHz 816 fs SMSR > 70 pulses from a mode-locked Er-fiber soliton laser by employing the technique of asynchronous phase modulation are presented in Chapter 3. In Chapter 4, long-term stabilization of the asynchronously mode-locked Er-fiber soliton laser is demonstrated by a simple and economic method based on the deviation-frequency extraction and locking. Chapter 5 describes the observation of new stable bound soliton pairs in a 10 GHz hybrid FM mode-locked Er-fiber laser. The mechanisms of bound state formation and the stability of these bound soliton pairs are investigated and discussed. Finally, Chapter 6 contains the conclusion of this research and discusses the possible research directions that can be pursued in the future.



References for Chapter 1:

- [1] L. E. Nelson, D. J. Jones, K. Tamura, H. A. Haus and E. P. Ippen, "Ultrashort-pulse fiber ring lasers," *Appl. Phys. B* **65**, 277 (1997).
- [2] H. A. Haus, "Mode-Locking of Lasers," *IEEE J. Selected Topics Quantum Electron.* **6**, 363 (2000).
- [3] U. Keller, "Recent developments in compact ultrashort lasers," *Nature* **424**, 831 (2003).
- [4] B. R. Washburn, S. A. Diddams, N. R. Newbury, J. W. Nicholson, M. F. Yan, C. G. Jorgensen, "Phase-locked, erbium-fiber-laser-based frequency comb in the near infrared," *Opt. Lett.* **29**, 1250 (2004).
- [5] T. R. Schibli, K. Minoshima, F.-L. Hong, H. Inaba, A. Onae, H. Matsumoto, I. Hartl, and M. E. Fermann, "Frequency metrology with a turnkey all-fiber system," *Opt. Lett.* **29**, 2467 (2004).
- [6] C. X. Yu, H. A. Haus, and E. P. Ippen, "Soliton squeezing at gigahertz rate in Sagnac loop," *Opt. Lett.* **26**, 669 (2001).
- [7] H. Lim, Y. Jiang, Y. Wang, Y.-C. Huang, Z. Chen, and F. W. Wise, "Ultrahigh-resolution optical coherence tomography with a fiber laser source at 1 μ m," *Opt. Lett.* **30**, 1171 (2005).
- [8] C. X. Yu, H.A. Haus, and E.P. Ippen, "Gigahertz-repetition-rate mode-locked fiber laser for continuum generation," *Opt. Lett.* **25**, 1418 (2000).
- [9] M. Nakazawa, and E. Yoshida, "A 40GHz 850-fs regeneratively FM mode-locked polarization-maintaining erbium fiber ring laser," *IEEE Photon. Technol. Lett.* **12**, 1613 (2000).
- [10] S. Watanabe, R. Okabe, F. Futami, R. Hainberger, C. Schmidt-Langhorst, C. Schubert, H. G. Weber, "Novel fiber Kerr-switch with parametric gain:

demonstration of optical demultiplexing and sampling up to 640 Gb/s,” in Proceedings of European Conference on Optical Communication (Stockholm, Sweden, 2004), Th4.1.6.

- [11] M. Nakazawa, H. Kubota, K. Suzuki, E. Yamada, and A. Sahara, “Ultra-high speed and long-distance TDM and WDM soliton transmission technology,” *IEEE J. Selected Topics Quantum Electron.* **6**, 363 (2000).
- [12] F. Ö Ilday, J. Chen, and F. X. Kärtner, “Generation of sub-100fs pulses at up to 200 MHz repetition rate from a passively mode-locked Yb-doped fiber laser,” *Opt. Express* **13**, 2716 (2005).
- [13] A. Ruehl, H. Hundertmark, D. Wandt, C. Fallnich, and D. Kracht, “0.7 W all-fiber Erbium oscillator generating 64 fs wave breaking-free pulse,” *Opt. Express* **13**, 6305 (2005).
- [14] J. R. Buckley, S. W. Clark, and F. W. Wise, “Generation of ten-cycle pulses from an ytterbium fiber laser with cubic phase compensation,” *Opt. Lett.* **31**, 1340 (2006).
- [15] N. G. Usechak, G. P. Agrawa, “FM Mode-Locked Fiber Lasers Operating in the Autosoliton Regime,” *IEEE J. Quantum Electron.* **41**, 735 (2005).
- [16] <http://www.imra.com/>.
- [17] J. Stone, C. A. Burrus, “Neodymium-doped silica lasers in end-pumped fiber geometry,” *Appl. Phys. Lett.* **23**, 388 (1973).
- [18] P. C. Becker, N. A. Olsson, J. R. Simpson “Erbium-Doped Fiber Amplifier,” Academic Press (1999).
- [19] V. J. Matsas, T. P. newson, D. J. Richardson, and D. N. Payne, “ Selfstarting passively mode-locked fibre ring soliton laser exploiting nonlinear polarization rotation,” *Electron. Lett.* **28**, 1391 (1992).
- [20] M. Hofer, M. E. Fermann, F. Haberl, M. H. Ober, and A. J. Schmidt, “Mode

- locking with cross-phase and self-phase modulation,” *Opt. Lett.* **16**, 502.
- [21] K. Tamura, H. A. Haus, and E. P. Ippen, “Self-starting additive pulse mode-locked erbium fiber ring laser,” *Electron. Lett.* **28**, 2226 (1992).
- [22] K. Tamura, E. P. Ippen, H. A. Haus, and L. E. Nelson, “77-fs pulse generation from a stretched-pulse mode-locked all-fiber ring laser,” *Opt. Lett.* **18**, 1080 (1993).
- [23] B. C. Collings, K. Bergman, T. Cundiff, S. Tsuda, J. N. Kutz, J. E. Cunningham, W. Y. Jan, M. Koch, and W. H. Knox, “Short cavity Erbium/Ytterbium Fiber Lasers Mode-Locked with a Saturable Bragg Reflector,” *IEEE J. Selected Topics Quantum Electron.* **3**, 1065 (1997).
- [24] H. A. Haus, J. G. Fujimoto, and E. P. Ippen, “Structure for additive pulse mode locking,” *J. Opt. Soc. Am. B* **8**, 2068 (1991).
- [25] H. A. Haus, E. P. Ippen, and K. Tamura, “Additive-Pulse Modelocking in Fiber Lasers,” *IEEE J. Quantum Electron.* **30**, 200 (1994).
- [26] K. Tamura, L. E. Nelson, H. A. Haus, and E. P. Ippen, “Soliton versus nonsoliton operation of fiber ring lasers,” *Appl. Phys. Lett.* **64**, 149 (1994).
- [27] G. T. Harvey and L. F. Mollenauer, “Harmonically mode-locked fiber ring laser with an internal Fabry-Perot stabilizer for soliton transmission,” *Opt. Lett.* **18**, 107 (1993).
- [28] Nakazawa, K. Tamura, and E. Yoshida, “Supermode noise suppression in a harmonically modelocked fiber laser by self phase modulation and spectral filtering,” *Electron. Lett.* **32**, 461 (1996).
- [29] X. Shan, D. Cleland and A. Ellis, “Stabilising Er fibre soliton laser with pulse phase locking,” *Electron. Lett.* **28**, 182-184 (1992).
- [30] J. W. Nicholson, A. D. Yablon, P. S. Westbrook, K. S. Feder, and M. F. Yan, “High power, single mode, all-fiber source of femtosecond pulses at 1550 nm and

its use in supercontinuum generation,” Opt. Express **13**, 3025(2004).

[31] <http://www.crystal-fibre.com/>

[32] L. F. Mollenauer, J. P. Gordon, and S. G. Evangelides, ”The sliding-frequency guiding filter: an improved form of soliton jitter control,” Opt. Lett. **17**, 1575 (1992).

[33] C. R. Doerr, H. A. Haus, and E. P. Ippen, “Asynchronous soliton mode locking,” Opt. Lett. **19**, 1958 (1994).

[34] W.-W. Hsiang, C.-Y. Lin, M.-F. Tien, and Y. Lai, “Direct generation of 10 GHz 816 fs pulse train from an erbium-fiber soliton laser with asynchronous phase modulation,” Opt. Lett. **30**, 2493 (2005).

[35] W.-W. Hsiang, C.-Y. Lin, and Y. Lai, “Stable new bound soliton in a 10 GHz hybrid frequency modulation mode-locked Er-fiber laser,” Opt. Lett. **31**, 1627 (2006).



Chapter 2

Soliton Phenomena in Passively Mode-Locked Er-Fiber Lasers

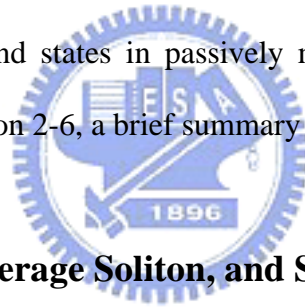
2.1 Introduction

Investigation and understanding of soliton phenomena were one of the most important works during the early stage development of passively mode-locked Er-fiber lasers. This is because soliton effects have a great influence both on the pulse width and pulse dynamics in passively mode-locked Er-fiber lasers [1-8]. For example, it is well known that in order to achieve shorter pulse width and higher pulse energy from mode-locked fiber lasers, the soliton regime operation should be replaced by the stretched pulse regime or parabolic pulse regime operation [2,9]. This is because that the soliton phenomena of resonant instability and spectral sidebands hinder the fiber laser in the soliton regime from obtaining the shortest pulse width corresponding to the Er-fiber gain bandwidth [2,5,6].

However, there are still other interesting soliton phenomena worthwhile to be studied and investigated in fiber soliton lasers. Recently, the multiple-pulse operation of fiber soliton lasers, i.e., more than one soliton simultaneously exist in the laser cavity, has attracted a lot of attention [10-15]. Multiple solitons occur in mode-locked fiber lasers due to the effects of soliton energy quantization when the laser gain exceeds the magnitude required for a single pulse operation. One example of multiple-soliton phenomena in fiber lasers is passive harmonic mode-locking, in which solitons are spaced orderly and equally in the laser cavity [10,12,13]. Another example is the soliton bound state. Multiple solitons are bound stably with the time

separation of only several hundred fs or several ps [11,14,15]. Both of these two examples mentioned above are related to the soliton-soliton interaction in passively mode-locked fiber lasers.

In this chapter, we will briefly review the basics of mode-locked fiber soliton lasers and the concepts introduced in this chapter will be used in the following chapters of the thesis. The concept of average soliton will be given based on the master equation for mode-locking. One of the main characteristics of fiber soliton lasers, i.e., spectral sidebands, will be described in Section 2-2. In Section 2-3, the effect of soliton energy quantization due to soliton area theorem and the saturation behavior of additive pulse mode-locking (APM) is introduced. Section 2-4 presents the experimental observations of passive harmonic mode-locking. The observation of various kinds of soliton bound states in passively mode-locked Er-fiber lasers are shown in section 2-5. In Section 2-6, a brief summary of this chapter is given.



2.2 Master Equation, Average Soliton, and Spectral Sidebands

Figure 2.1 shows the schematic diagram of P-APM (polarization additive pulse mode-locking) Er-fiber laser. The Er-fiber laser is equivalent to a ring cavity with gain, loss, group velocity dispersion (GVD), self phase modulation (SPM), and self amplitude modulation (SAM) [8]. SAM represents the effects of an artificial fast saturable absorber, which can be achieved by P-APM. Figure 2.2 illustrates the principle of P-APM [16]. The polarizer and wave plate will set the incident light at a suitable elliptical polarization. The third-order nonlinearity of the fiber, i.e., SPM and cross phase modulation (XPM), will cause the nonlinear rotation of elliptical polarization such that the light with higher intensity experiences less loss than the light with weaker intensity when they pass through the polarizer.

The passively mode-locked Er-fiber laser can be modeled by the master equation by [8,16,17]

$$T_R \frac{da(t,T)}{dT} = [-l + g(1 + \frac{l}{\Omega_g^2}) \frac{d^2}{dt^2} + jD \frac{d^2}{dt^2} + (\gamma - j\delta) |a(t,T)|^2] a(t,T). \quad (2.1)$$

where T_R is the round trip time; $a(T,t)$ is the field envelope of the pulse, with a short-term time variable t and a long-term time variable T on the scale of cavity round trip time T_R ; l represents the loss; g is the gain; Ω_g is the gain bandwidth; γ and δ are coefficients of SAM and SPM respectively; D is the group velocity dispersion coefficient. The sign of γ must be positive such that higher intensity sees less loss.

It has been shown that the soliton solutions (strictly speaking, chirp-free solitary pulses) can be obtained from Eq. (2.1) when the signs of D and δ are opposite, and the gain dispersion and APM action are related to SPM and anomalous GVD by

$$\frac{D}{\delta} = -\frac{g/\Omega_g^2}{\gamma}. \quad (2.2)$$

Therefore in the laser cavity with anomalous GVD and SPM, one can obtain the chirp-free solitary solution [17], which can be represented by

$$a(t,T) = A_0 \operatorname{sech}\left(\frac{t}{\tau}\right) \exp\left(-j \frac{\delta A_0^2}{2} \frac{T}{T_R}\right) \quad (2.3)$$

with the following two relations

$$\tau = \frac{l}{A_0} \sqrt{\frac{2|D|}{\delta}} \quad (2.4)$$

$$g - l = -\frac{l}{\tau^2} \frac{g}{\Omega_g^2} = -\frac{\gamma}{2} A_0^2. \quad (2.5)$$

One can note that the chirp-free solitary solution of Eq. (2.3) is equal to the fundamental soliton obtained from nonlinear Schrödinger equation with the same parameters of D and δ . Since the master equation describes the average effect of

the laser cavity, therefore the solution of (2.3) is an average soliton over the cavity round trip. Actually, when the solitons propagate along the fiber laser, they are periodically perturbed and the dispersive waves will shed from the perturbed solitons [2,5,6]. The dispersive waves can be resonant with solitons and can strongly build up

at the frequencies of $\Delta\omega = \pm \frac{1}{\tau} \sqrt{m \frac{8Z_0}{Z_p} - 1}$, where $Z_0 = \frac{\pi\tau^2}{2|\beta_2|}$ is soliton period,

Z_p is the cavity length, m is integers, and $\Delta\omega$ is the frequency offset from the center frequency spectrum [18]. These peaks on the optical spectrum, i.e., spectrum sidebands (also called Kelly sidebands [5]), are the main characteristics of fiber soliton lasers. The phenomena of resonant instability ($m=0$) and spectral sidebands ($m \neq 0$) hinder the fiber laser in the soliton regime from obtaining the shortest pulse width corresponding to the Er-fiber gain bandwidth.

In section 2-4, we will see the clear spectrum sidebands when the passively mode-locked Er-fiber laser is in the soliton regime. On the contrary, the spectrum sidebands do not appear when the same mode-locked Er-fiber laser operates in the stretched pulse regime.

2.3 Saturation of APM and Soliton Energy Quantization

On one hand, Equation (2.4) indicates the area theorem of fiber soliton lasers [17].

The product of pulse amplitude and pulse width will remained as a constant of

$\tau A_0 = \sqrt{\frac{2|D|}{\delta}}$. On the other hand, the saturation of P-APM needs to be considered

when the pulse amplitude becomes stronger and stronger. Because P-APM is based on

the nonlinear interference, the term of SAM in the master equation (2.1) can be

presented more accurately by $\sin(\gamma|u|^2)$ [16,18]. When the pulse shape $a(t)$ is in

the shape of $a(t) = A_0 \operatorname{sech}(t/\tau)$, the gain which can be acquired from P-APM is

$$\int_{-\infty}^{\infty} |a|^2 \sin(\gamma |a|^2) dt .$$

When the soliton area theorem is included, the maximum gain

acquired from P-APM is $\gamma |A_0|^2 \cong 0.6\pi$. Therefore the maximum of pulse amplitude

A_0 as well as soliton pulse energy $2A_0^2\tau$ are limited. This indicates the effect of

soliton energy quantization. The phenomenon of soliton energy quantization is

observed when the fiber laser have the excessive gain or when the fiber laser has a

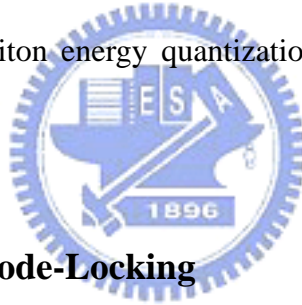
large SAM coefficient γ due to the long cavity length of fiber laser. In the following

section, we describe the observation on passive harmonic mode-locking in a P-APM

Er-fiber laser [19]. The spontaneous repetition rate multiplication is one of the soliton

phenomena resulted from soliton energy quantization and related to soliton-soliton

interaction.



2.4 Passive Harmonic Mode-Locking

Passively mode-locked Er-fiber lasers have been developed for more than one decade

and can generate ultrashort optical pulse in the femtosecond time scale[18]. Although

sub-picosecond pulse can be obtained easily from passively mode-locked fiber lasers,

the pulse repetition rate is usually quite low due to their long cavity length. The cavity

length of passively mode-locked fiber lasers is typically from several tens of meters to

several meters, and thus the corresponding pulse repetition rate is from several MHz

to nearly 100 MHz. For some applications, such a low pulse repetition rate has

discouraged the usage of passively mode-locked fiber laser. Several methods have

been proposed to increase the pulse repetition rate of passively mode-locked fiber

laser, such as: (1) reduce the total cavity length to several meters or even shorter [20];

(2) combination of active harmonic mode-locking to build hybrid mode-locked fiber laser [21]; (3) Adoption of passive pulse repetition rate multiplication schemes in the cavity or outside the cavity [22,23]. In this section, we report on the observation of various interesting pulse dynamics in a P-APM Er-fiber laser [19]. Under suitable adjustments, dynamic processes of pulse-splitting, pulse bunch formation as well as stable passive harmonic mode-locking have been observed. At the same pump power and with suitable adjustment of the polarization controllers, the laser can switch between operating at the fundamental repetition rate as a stretched-pulse P-APM laser and operating at higher harmonic repetition rates (as high as 34) as a soliton laser. We find that the characteristics of laser pulses at the fundamental repetition rate and at higher harmonic repetition rates seems to be quite different. At the fundamental repetition rate, the laser pulse has a shorter pulse-width and is not a soliton in the cavity whereas at higher harmonic repetition rates the laser pulse inside the cavity has a longer pulse-width and is a soliton as indicated by the clearly observed sideband peaks in its optical spectrum.

The schematic of our experimental setup is shown in Fig. 2-3. The P-APM Er-fiber laser consists of two polarization controllers and one polarization dependent isolator. The total cavity length is about 20 m long, which comprises of a 3 m Er-doped fiber with a group velocity dispersion of -45 ps/ nm km and 17 m single mode fiber with a group velocity dispersion of 17 ps/ nm km. The laser is pumped by the semiconductor laser at the wavelength of 980 nm. By adjusting two polarization controllers, self-starting operation can be easily achieved at the fundamental pulse repetition rate when the pump power is larger than 150 mW. When the laser operates at the fundamental pulse repetition rate, pulse width less than 500 fs can be easily obtained. The optical spectrum of the output pulse at the fundamental pulse repetition rate is shown in Fig. 2-4(a), which has the bandwidth of 54 nm and a central

wavelength of 1566 nm. The output power of the laser is 5.25 mW and the fundamental pulse repetition rate is 10.2 MHz. When the polarization controller is further suitably adjusted with the pump power fixed, the stable mode-locking operation at the fundamental repetition rate can be made to disappear and the laser can be switched to operate at a higher harmonic repetition rate. From the RF spectrum analyzer and the fast oscilloscope connected to a fast photodiode for monitoring the optical pulse, we can see the whole dynamic process of pulse-splitting, pulse bunch formation, and finally self-stabilized passive harmonically modelocking. Figure 2-5 shows the RF spectra of these three different processes. The typical optical spectrum of the pulses after switching to the higher harmonic repetition rate is shown in Fig. 2-4(b). As one can see, several spectral sidebands appear apparently, which indicates that the pulses inside the cavity are solitons with a subpicosecond pulse width after switching to the higher harmonic repetition rate [3, 5, 6]. This is totally different from the case when the laser operates at the fundamental pulse repetition rate.

The output power of the laser changes very little when switching between the two regimes, which indicates that the pulse energy at the fundamental repetition rate is redistributed equally into many pulses after switching to the higher repetition rate. Fig 2-6(a) shows the RF spectra at the 4, 25, and 34 harmonic repetition rate, which indicates stable mode-locking has been achieved. We also find that our laser can operate at different harmonic pulse repetition rates from 4 to 34 when the pump power is changed, as shown in Fig. 2-6(b). When the output power, or correspondingly the pump power is low, the laser behaves like a soliton laser such that the pulse repetition rate increases linearly with the output power. However, when the pump power is too high, irregular behaviors occur and it is difficult to achieve a higher harmonic repetition rate. The threshold power for self-starting harmonic modelocking is about the pump power for the 14-th harmonic. In our experiment the lower harmonic

mode-locking states are reached by decreasing the pump power after achieving the self-started 14-th harmonic repetition rate.

The interesting phenomena mentioned above are closely related to the physics of the P-APM mechanism and the soliton pulse propagation dynamics inside the cavity. Since our net cavity dispersion is in the anomalous regime, the formation of average-solitons or guiding-center solitons inside the fiber laser cavity becomes possible. The role played by the P-APM mechanism is to shorten the pulse for achieving the modelocking. When our laser is operating at the fundamental pulse repetition rate, the pulse energy is much higher than that of the fundamental soliton calculated from the net cavity dispersion. We think this is because the pulse-width at this operation state is short enough for the stretched-pulse mechanism to become important and thus at this operation state the optical pulse inside the cavity does not behave like a soliton. Another supporting proof is that the characteristic sideband peaks of a soliton laser do not show up at this operation state. With suitable adjustment of the polarization controllers, it is possible to lower the APM threshold intensity and force the initial pulse to break into a series of smaller pulses and finally the harmonic mode-locking is achieved. The pulse width at this new state is a little longer due to the decreasing of APM pulse-shortening force and thus the soliton characteristics of the laser pulse will become more apparent at this operating state. In the following the formation of multiple pulses inside one round trip can be understood by the soliton energy quantization and the mechanisms for finally stabilizing the laser can be due to several possible factors including the acoustic-optic effects, the interaction between soliton pulses and the continuum, and the dynamic gain depletion [24-26]. The reason why the dependence of the harmonic number on the pump/output power becomes irregular for high pump power could be that the dispersive wave shed by the periodically perturbed solitons will affect seriously the multiple pulse

formation dynamics [3,26]. With the dispersive waves growing up, the pulse repetition rate can not be controlled directly by changing the pump power simply because the gain is not only depleted by the multiple solitons but also by the strong dispersive waves.

2.5 Soliton Bound States

In this section, the experimental observations of soliton bound states in the passively mode-locked Er-fiber laser are shown. Instead of the equal time separations of several tens ns to several ns between the solitons in passive harmonic mode-locking, the time separations between the bound solitons are only several hundred femtoseconds to several picoseconds. Figure 2-7 shows the SHG autocorrelation trace of the soliton bound states with ps time separations, and the respective optical spectrum is shown in Fig. 2-8. In Fig. 2-7, a variety of soliton bound states has been observed, including two identical bound solitons, five identical bound solitons with equal spacing, and three bound solitons with unequal spacing. For the femtosecond soliton pulse, separation of several ps indicates that these solitons do not overlap and the long-range interaction exists to maintain the bound solitons stably. The long-range interaction may be resulted from the effects of dispersive waves, gain relaxation, and acoustic wave in fiber lasers [24-26].

Bound solitons with the time separation of a few hundred femtoseconds are also observed in the same passively mode-locked Er-fiber laser. In Fig. 2-9, the SHG autocorrelation trace shows the time separation between the bound soliton pair is less than 1 ps. Fig. 2-10 shows the optical spectrum of this closely bound soliton pair with the larger modulation period compared to Fig. 2-8. The closely bound solitons can

interact each other by the overlap of the tails of the pulses, and this soliton bound states can be modeled by Ginzberg-Landau equations within certain parameter regimes [11,27].

2.6 Summary

In this chapter, based on the master equation of passively mode-locked lasers, we introduce the concept of average soliton in the mode-locked Er-fiber laser. The experimental observations of soliton energy quantization and spectral sidebands show the main characteristics of P-APM Er-fiber lasers in soliton regime. Although in soliton regime the passively mode-locked Er-fiber lasers can not generation pulses as short as the pulses from stretched pulse regime, the occurrence of multiple pulses still exhibits exotic soliton phenomena, such as passive harmonic mode-locking and soliton bound states. The passive harmonic mode-locking shows the capability of increasing the repetition rates of femtosecond Er-fiber soliton lasers. However, the repetition rates of spontaneous multiplication are limited to several hundreds of MHz in our case. Besides, the harmonic of spontaneous multiplication is usually not easy to precisely control, and typically passive harmonic mode-locking does not own a very high supermode noise suppression ratio (SMSR). In order to solve these problems, we adopt the method of asynchronous soliton mode-locking to generate high repetition rate femtosecond pulses, and this part will be described in Chapter 3 and Chapter 4. At the end of this chapter, the observations of various soliton bound states in the P-APM Er-fiber laser are shown. In the literature, soliton bound states in passively mode-locked fiber lasers have been intensely investigated, and a lot of efforts have been dedicated to explain and understand these soliton phenomena. However, it is still an academic interest to ask and explore the possibility of the existence of any other

soliton bound states from the different kinds of mode-locked fiber lasers. The works of the observations of the new soliton bound state in hybrid FM mode-locked Er-fiber laser will be presented in Chapter 5.



References for Chapter 2:

- [1] D. J. Richardson, R. I. Laming, D. N. Payne, M. W. Phillips, and V. J. Matsas, “320 fs soliton generation with passively mode-locked erbium fibre laser,” *Electron. Lett.* **27**, 730 (1992).
- [2] K. Tamura, L. E. Nelson, H. A. Haus, and E. P. Ippen, “Soliton versus nonsoliton operation of fiber ring lasers,” *Appl. Phys. Lett.* **64**, 149 (1994).
- [3] S. M. J. Kelly, K. Smith, K. J. Blow, N. J. Doran, “Average Soliton Dynamics of a High-Gain Erbium Fiber Laser,” *Opt. Lett.* **16**, 1337 (1991).
- [4] K. Tamura, E. P. Ippen, and H. A. Haus, “Optimization of Filtering in Soliton Fiber Laser,” *IEEE Photon. Technol. Lett.* **6**, 1433 (1994).
- [5] S. M. J. Kelly, “Characteristic sideband instability of periodically amplified average soliton,” *Electron. Lett.* **28**, 806 (1992).
- [6] N. Pandit, D. U. Noske, S. M. J. Kelly, and J. R. Taylor, “Characteristic instability of fibre loop soliton lasers,” *Electron. Lett.* **28**, 455 (1992).
- [7] V. J. Matsas, T. P. Newson, D. J. Richardson, and D. N. Payne, “Selfstarting passively mode-locked fibre ring soliton laser exploiting nonlinear polarization rotation,” *Electron. Lett.* **28**, 1391 (1992).
- [8] H. A. Haus, J. G. Fujimoto, and E. P. Ippen, “Structure for additive pulse mode locking,” *J. Opt. Soc. Am. B* **8**, (1991).
- [9] J. R. Buckley, F. W. Wise, F. Ö. Ilday, and T. Sosnowski, “Femtosecond fiber lasers with pulse energies above 10 nJ,” *Opt. Lett.* **30**, 1888 (2005).
- [10] A. B. Grudinin and S. Gray, “Passive Harmonic Mode locking in Soliton Fiber Laser,” *J. Opt. Soc. Am. B* **14**, 144, (1997).

- [11] D. Y. Tang, W. S. Man, H. Y. Tam, and P. D. Drummond, "Observation of bound states of solitons in a passively mode-locked fiber laser," *Phys. Rev. A* **64**, 033814 (2001).
- [12] S. Zhou, D. G. Ouzounov, and F. W. Wise, "Passive harmonic mode-locking of a soliton Yb fiber lasers at repetition rate to 1.5 GHz," *Opt. Lett.* **31**, 1041 (2006).
- [13] D. Panasenko, P. Polynkin, A. Polynkin, J. V. Moloney, M. Mansuripur, and N. Peyghambarian, "Er-Yb Femtosecond Ring Fiber Oscillator With 1.1-W Average Power and GHz repetition Rates," *IEEE Photon. Technol. Lett* **18**, 853 (2006).
- [14] J. M. Soto-Crespo, N. Akhmediev, P. Grelu, and F. Belhache, "Quantized separations of phase-locked soliton pairs in fiber lasers," *Opt. Lett.* **28**, 1757 (2003)
- [15] M. Oliver, V. Roy, and M. Piché, "Third-order dispersion and bound states of pulses in a fiber laser," *Opt. Lett.* **31**, 580 (2006).
- [16] H. A. Haus, E. P. Ippen, and K. Tamura, "Additive-Pulse Modelocking in Fiber Lasers," *IEEE J. Quantum Electron.* **30**, 200 (1994).
- [17] H. A. Haus and A. Mecozzi, "Noise of Mode-Locked Lasers," *IEEE J. Quantum Electron.* **29**, 983 (1993).
- [18] L. E. Nelson, D. J. Jones, K. Tamura, H. A. Haus and E. P. Ippen, "Ultrashort-pulse fiber ring lasers," *Appl. Phys. B* **65**, 277 (1997).
- [19] W.-W. Hsiang, C.-C. Chung and Y. Lai, "Observation of Pulse Repetition Rate Multiplication in a Stretched-Pulse Additive-Pulse-Modelocking Er-Fiber Laser," Paper TU3G (6)-4, CLEO/Pacific-Rim 2003, Taipei, Taiwan.
- [20] S. Yamashita, Y. Inoue, K. Hsu, T. Kotake, H. Yaguchi, D. Tanaka, M. Jablonski, S. Y. Set, "5-GHz pulsed fiber Fabry-Perot laser mode-locked using carbon nanotubes," *IEEE Photon. Technol. Lett* **17**, 750 (2005).
- [21] C. X. Yu, H.A. Haus, and E.P. Ippen, "Gigahertz-repetition-rate mode-locked

- fiber laser for continuum generation,” *Opt. Lett.* **25**, 1418 (2000).
- [22] J. T. Ahn, H.K. Lee, K.H. Kim, M.Y. Jeon, E. H. Lee, “A Passively Mode-locked Fiber Laser with a Delayed Optical Path for Increasing the Repetition Rate,” *Opt. Commun.* **148**, 59 (1998).
- [23] T.-M. Liu, F. X. Kärtner, J. G. Fujimoto, and C.-K. Sun, “Multiplying the repetition rate of passive mode-locked femtosecond lasers by an intracavity flat surface with low reflectivity,” *Opt. Lett.* **30**, 439 (2005).
- [24] K. S. Abedin, J. T. Gopinath, L. A. Jiang, M. E. Grein, H. A. Haus, and Erich P. Ippen, “Self- stabilized Passive, Harmonically Mode-locked Stretched-pulse Erbium Fiber Ring Laser,” *Opt. Lett.* **27**, 1758 (2002).
- [25] B. C. Collings, K. Bergman, and W. H. Knox, “Stable multigigahertz pulse-train formation in a short-cavity passively harmonic mode-locked erbium/ytterbium fiber laser,” *Opt. Lett.* **23**, 123 (1998).
- [26] J. P. Gordon, “Dispersive perturbation of solitons of the nonlinear Schrödinger equation,” *J. Opt. Soc. Am. B* **9**, (1992).
- [27] N. N. Akhmediev, A. Ankiewicz, and J. M. Soto-Crespo, “Multisoliton Solutions of the Complex Ginzburg-Landau Equation,” *Phys. Rev. Lett.* **79**, 4047-4051 (1997).

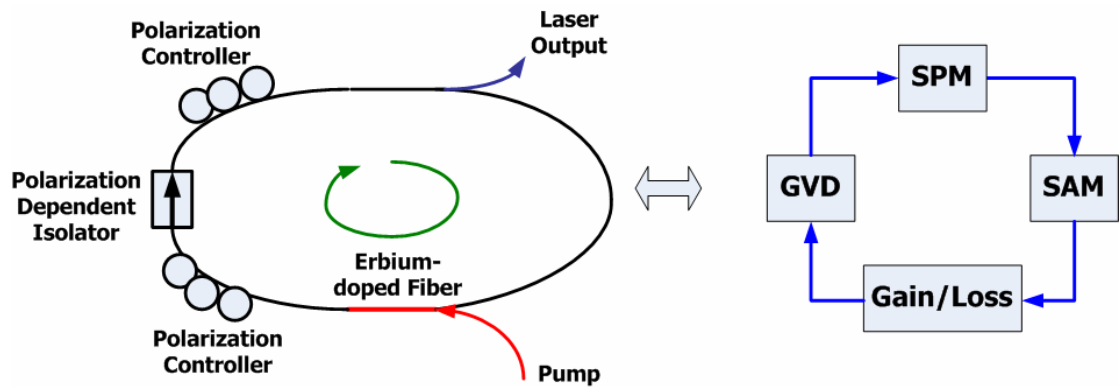


Fig. 2-1 Left: schematic diagram of the P-APM fiber laser. Right: equivalent ring cavity of the P-APM fiber laser.

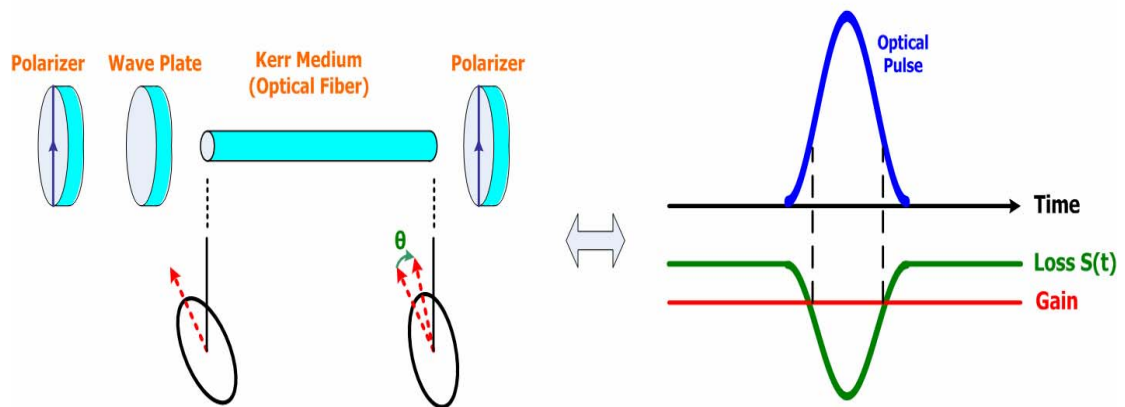


Fig. 2-2 Left: illustration of nonlinear rotation of elliptical polarization of P-APM. Right: the effect of saturable absorber achieved by P-APM.

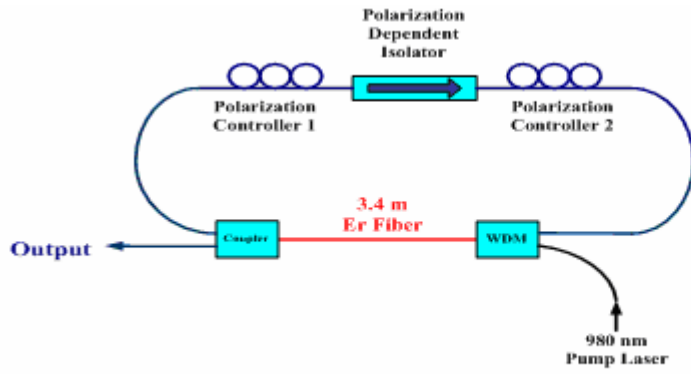
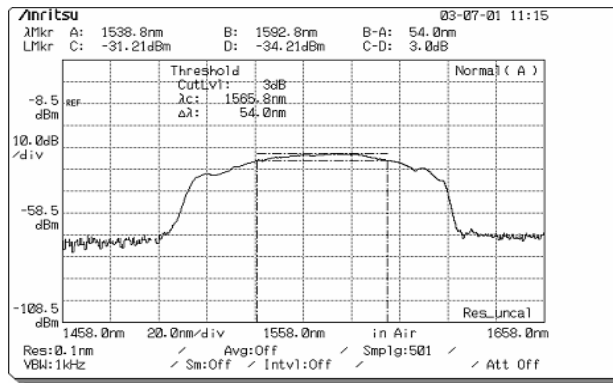
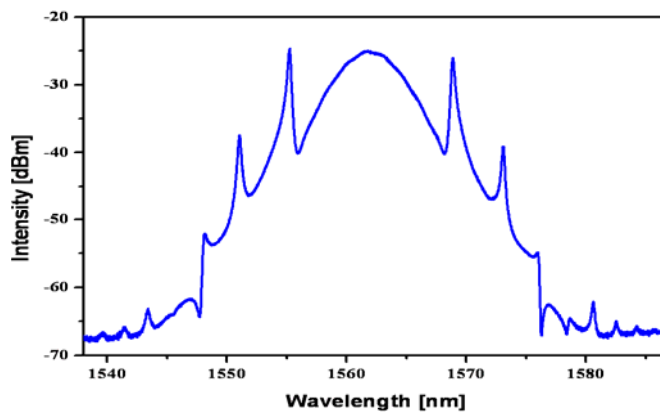


Fig. 2-3 Schematic diagram of experimental setup.

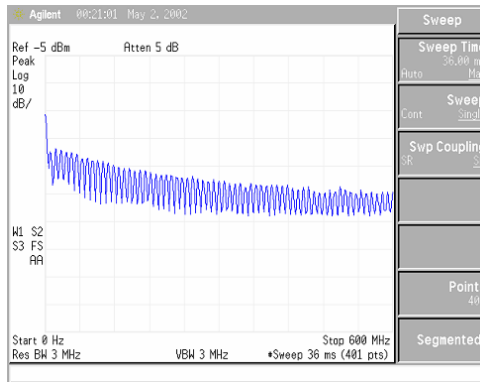


(a)

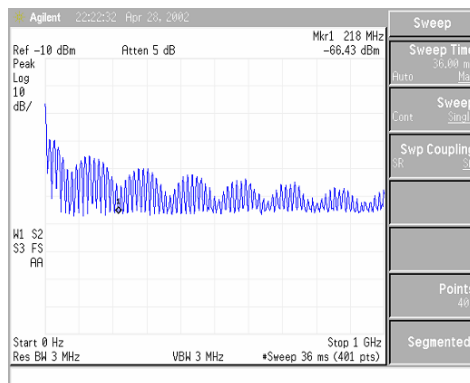


(b)

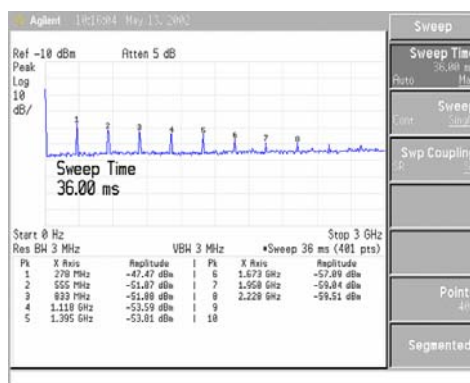
Fig. 2-4 Optical spectra of the two different mode-locking regimes of a P-APM Er-fiber laser. (a) Stretched pulse regime at fundamental repetition rate (b) Soliton regime at harmonic repetition rates.



(a)

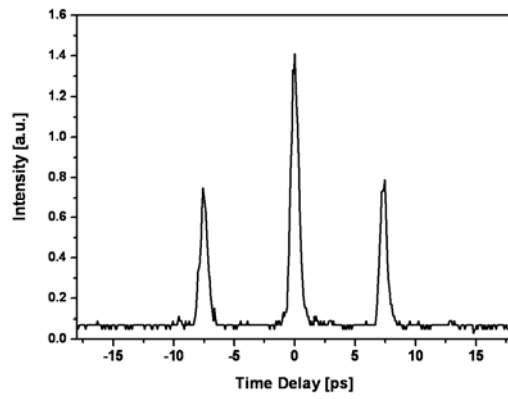


(b)

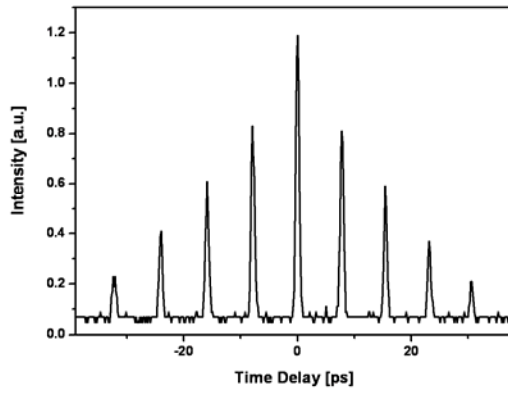


(c)

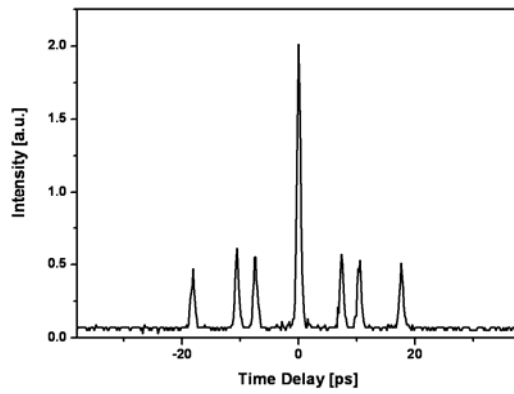
Fig. 2-5 The RF spectra when the spontaneous pulse repetition rate multiplication occurs. (a) At beginning: fundamental repetition rate (b) Pulse bunching (c) Passive harmonic mode-locking.



(a)



(b)



(c)

Fig. 2-7 SHG autocorrelation trace of the different soliton bound states with ps time separation. (a) Two identical bound solitons (b) Five identical bound solitons with the same time separation (c) Three bound solitons with the different time separations.

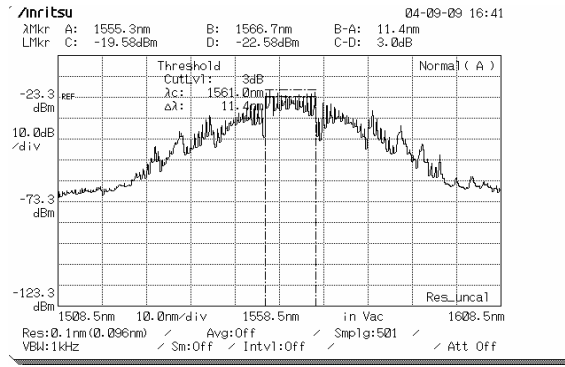


Fig. 2-8 Optical spectrum of the soliton bound states with ps time separation.

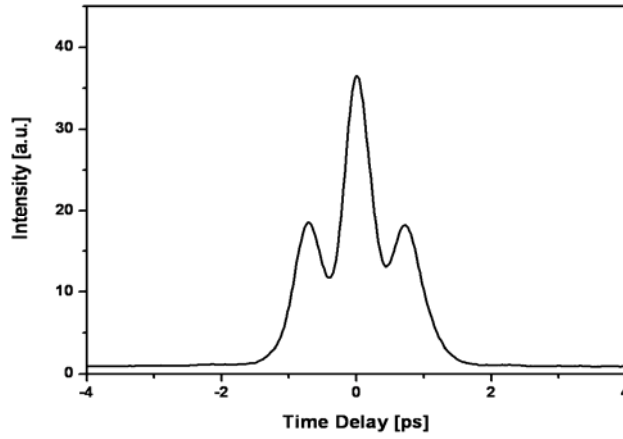


Fig. 2-9 SHG autocorrelation trace of the bound soliton pair with fs time separation.

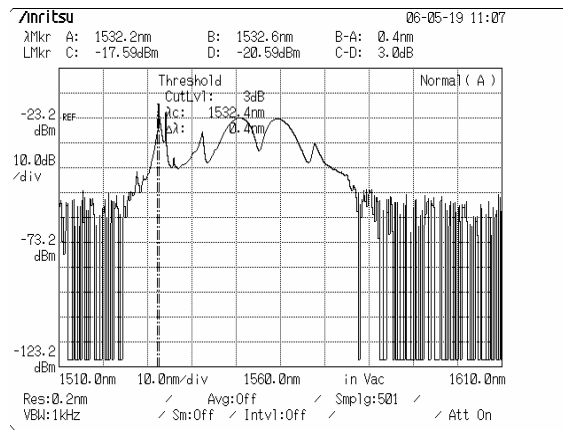


Fig. 2-10 Optical spectrum of the bound soliton pair with fs time separation.

Chapter 3

10 GHz 0.8 ps Asynchronously Mode-Locked Er-Fiber Soliton Laser

3.1 Introduction

Ultra-short laser pulse sources with a high repetition rate are desirable for various applications including high speed optical communication [1], ultra-fast optical sampling [2], optical continuum generation [3,4] and quantum optics experiments like squeezed state generation [5]. In previous chapter, we have shown that the repetition rates of femtosecond passively mode-locked Er-fiber lasers are typical less than 100 MHz due to the long cavity length. Although passive harmonic mode-locking is able to increase the pulse repetition rate, the multiplication factors in fiber soliton lasers is usually not high enough for practical applications. In addition, it is still difficult to precisely control the multiplication factors when the spontaneous repetition rate multiplication occurs.

Mode-locked Er-fiber lasers with high repetition rates up to a few tens of GHz can be achieved by the technique of active harmonic mode-locking. Although optical pulses from actively mode-locked fiber lasers can be transform-limited and even with quantum-limited timing jitter [6], their pulse widths are typically in the picosecond range when the modulation frequency is less than 40 GHz [7-9]. Thus, additional pulse compression mechanisms outside the laser cavity are needed to obtain shorter pulse width [8]. The technique of hybrid mode-locking has been identified as a possible solution for directly generating femtosecond pulses at a high repetition rate [3,10]. In these lasers, the mechanism of passive mode-locking is also utilized to

further shorten the pulse width. However, there are still very few reports, if any, on the success of directly generating femtosecond pulses at 10GHz or higher.

In the literature, one interesting mode-locking mechanism is the asynchronous modulation hybrid soliton modelocking technique which utilizes the optical carrier frequency sweeping effect caused by asynchronous phase modulation to clean up the noise through the equivalent sliding guiding-center soliton effect. Such a technique has been used to produce pulse trains with 1-ps pulsewidth at 1-GHz repetition rate [11]. In principle, the asynchronous mode-locking technique can be further developed to generate shorter pulse trains at higher repetition rates [12,13].

In this chapter we explore this possibility and successfully demonstrate a femtosecond mode-locked Er-fiber soliton laser at 10 GHz repetition rate by asynchronous phase modulation [14]. In Section 3.2, we briefly review the basic principle of asynchronous soliton mode-locking and illustrate the reasons why we can obtain the advantages of high supermode noise suppression ratio (SMSR) and shorter pulse width from this mode-locking technique. The experimental setup of the asynchronously mode-locked Er-fiber soliton laser is described in Section 3.3, and the experimental results of direct generation of 10 GHz 816 fs SMSR > 70 dB pulses from asynchronously mode-locked Er-fiber laser is presented in Section 3.4. Finally, Section 3.5 includes the discussion and summary.

3.2 Asynchronous Soliton Mode-Locking

In normal active or harmonic mode-locking, the optical modulator in the laser cavity is driven synchronously, i.e., the modulation frequency is exactly equal to the cavity frequency or cavity harmonic frequency. The pulses will be mode-locked at the center of the amplitude modulation (AM) cycles due to the less loss or at the center of the

down/up chirped frequency modulation (FM) cycles due to the zero frequency shift [15, 16]. However, in mode-locked Er-fiber laser, asynchronous soliton mode-locking can be achieved when the phase modulator is driven asynchronously, i.e., the modulation frequency is detuned from the cavity harmonic frequency by several KHz to several tens of KHz [11-14]. The principle and advantages of asynchronous soliton mode-locking are illustrated as follows.

The basic principle of asynchronous soliton mode-locking can be understood from Fig. 3-1(a). Figure 3-1(a) shows the soliton in the ring cavity with the gain, the filter, group velocity dispersion (GVD), self phase modulation (SPM) and the phase modulator driven asynchronously. Because of asynchronous modulation, the optical pulse passing through the phase modulator will obtain a frequency shift $\Delta\omega_{ASM}$ due to the timing difference Δt_{ASM} between the pulse and the modulation signal. For the linear pulse, it will follow the asynchronous phase modulation and thus have the relatively large displacement of optical carrier frequency. Due to the limited bandwidth of the gain and the optical filter, the linear pulse will experience a huge loss and can not exist in the asynchronously mode-locked fiber laser. However, on the contrary, the soliton can resist the displacement of the frequency shifts induced by asynchronous modulation and experience less loss than linear pulses, since the carrier frequency of solitons will keep following the center wavelength of the gain or the filter. Effectively, for solitons in asynchronous mode-locking, there exists an additional frequency shift $\Delta\omega_{soliton}$ to draw the carrier frequency of soliton back to the center wavelength of the filter or the gain in the laser. This effect is equivalent to the sliding-frequency guiding filters used in soliton fiber communication [17,18]. The solitons in the optical fiber link will follow the center wavelength of the sliding filter, but the linear noises will be filtered out due to the cascaded filters with sliding center wavelengths.

The phenomenon of asynchronous soliton mode-locking can be analyzed by soliton perturbation theory [12,19]. The equations of motion for the frequency displacement $\Delta\omega$ and the time displacement Δt of the perturbed soliton with asynchronous phase modulation are described by

$$T_R \frac{d\Delta\omega}{dT} = -\frac{\Delta\omega}{\tau_0} + S_p T_R \quad (3.1)$$

$$T_R \frac{d\Delta t}{dT} = 2 |D| \Delta\omega \quad (3.2)$$

$$\frac{1}{\tau_0} = \frac{4}{3} \frac{g_{eff}}{\Omega_{g,eff}^2 \tau_s^2} \quad (3.3)$$

$$S_p T_R = -M \Omega_M \sin(\Delta\Omega T) \quad (3.4)$$

where T_R is the round trip time; T is a long-term time variable on the scale of cavity round trip time T_R ; D is the group velocity dispersion coefficient; τ_s is the soliton pulse width; $S_p T_R$ represents the effect of asynchronous phase modulation ; M is the modulation depth; $\Delta\Omega$ is the deviation frequency between the modulation frequency Ω_M and cavity harmonic frequency.

One can clearly see that there exists a recovery effect of $-\frac{\Delta\omega}{\tau_0}$ in the equation of motion for the frequency displacement due to the filtering effects of the gain and the filter. This is why the carrier frequency of the soliton will follow the center frequency of the filter. On the contrary, the linear pulse dose not own this decay term in the equation of motion for the frequency displacement. The two equations (3.1) and (3.2) also show that there are slow periodical modulations both on the soliton carrier frequency and the soliton timing position in asynchronous mode-locking. When the rate of change of $\Delta\omega$ is much slower than $\frac{1}{\tau_0}$, one can obtain the frequency displacement $\Delta\omega$ and the time displacement Δt of the perturbed soliton described by

$$\Delta\omega \approx -\tau_0 M \Omega_M \sin(\Delta\Omega T) \quad (3.5)$$

$$\Delta t \approx \frac{2|D|(\tau_0 M \Omega_M)}{\Delta\Omega} \cos(\Delta\Omega T). \quad (3.6)$$

The slow modulation property of soliton timing position Δt and soliton carrier frequency $\Delta\omega$ is one of the main characteristic of asynchronous mode-locking, as shown in Fig. 3-1(b).

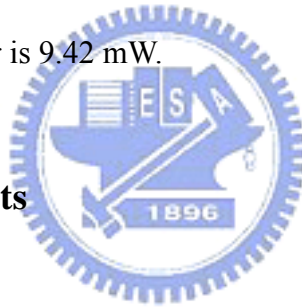
On one hand, asynchronous soliton mode-locking provides one feasible method to form stable soliton pulse when an active modulator is used to increase the repetition rate. Because the pulse width of soliton is determined by the laser cavity parameters, instead of the phase modulator, we can obtain shorter pulse width when compared to the pulses by synchronous mode-locking. On the other hand, as shown in Fig. 3-1(c), linear noises will have a large frequency displacement and experience more loss from the filtering effect. It provides another advantage for asynchronous mode-locking: a higher SMSR can be obtained, even when there is no explicit intracavity optical devices to suppress the supermode noise [20].

3.3 Experimental Setup

Our experimental setup of asynchronously mode-locked Er-fiber laser is shown in Fig. 3-2. The fiber laser consists of a LiNbO₃ phase modulator, two polarization controllers, an isolator, two WDM couplers, an output coupler, a tunable optical filter with FWHM=14nm, a section of 6-m Er-fiber ($\beta_2: 57 \text{ ps}^2 / \text{km}$), and two 980-nm pump laser diodes. No polarization beam splitter or polarization-dependent isolator is used in the setup, since the phase modulator we use has enough polarization dependent loss difference for acting as a polarizing element in the polarization rotation additive-pulse mode-locking (P-APM) mechanism. This is proved by the fact

that we can observe stable femtosecond pulse train at the cavity fundamental repetition rate when the phase modulator is off. A total pump power up to 800 mW has been used to pump the Er-fiber. The optical bandpass filter can cooperate with the SPM to get higher SMSR [21]. It also offers the filtering mechanism required for noise clean-up through the equivalent sliding-filter guiding-center soliton effect caused by asynchronous mode-locking [12]. The output fiber coupler couples 30% of the cavity power to the output port and a 1.5-m dispersion shift fiber (DSF) is used to avoid output pulse broadening. No noticeable spectrum broadening effect caused by the DSF is observed in our case. The total length of the laser cavity is 24.9 m and its corresponding fundamental repetition rate is 8.3 MHz. The average cavity dispersion parameter β_2 is estimated to be $-2.26 \text{ ps}^2/\text{km}$. When the laser is pumped with 735mW pump power, the output power is 9.42 mW.

3.4 Experimental Results



We have observed that there are two types of possible pulse operation states for our mode-locked laser: the linear Gaussian pulse state and the nonlinear soliton pulse state. Whether one can obtain the solitons or the Gaussian pulses is determined by the modulation frequency (asynchronous or synchronous). On one hand, by detuning the deviation of the modulation frequency from the cavity harmonic frequency about 15~40 kHz (asynchronous mode-locking), the soliton pulses are formed. On the other hand, the Gaussian pulses are formed when the laser is mode-locked with synchronous modulation. With operated asynchronously, the laser can produce sub-picosecond pulses train at 10-GHz repetition rate, despite the asynchronous timing between the pulses and the modulation signal. The output pulse train is stable

and with a high SMSR (more than 70 dB, limited by the detection equipment). Figure 3-3(a) shows the optical spectrum of the mode-locked laser output with asynchronous modulation. The FWHM spectral bandwidth is 3.24 nm. The corresponding SHG autocorrelation trace is shown in Fig. 3-3(b) and the pulse width from hyperbolic secant fitting is 816 fs. The time-bandwidth product is 0.32, indicating that the pulses are with little chirp. Fig. 3-4 shows the RF spectra of the signals from the fast photodetector connected to the laser output. In Fig. 3-4(a), the RF spectrum near 10 GHz is shown with 20 MHz span, which covers almost 3 times of the cavity frequency. Except the main peak near 10 GHz, no signal at other cavity harmonic frequencies is observed, indicating the SMSR is more than 70 dB. In Fig. 3-4(b), the same RF spectrum is shown with the smaller span of 200 kHz. The 1204th harmonic cavity frequency is 9.997727 GHz and the modulation frequency is 9.997763 GHz. The detuning between the modulation frequency and cavity harmonic frequency can be clearly observed through the beating signals with the spectral spacing equal to the frequency deviation of 36 kHz. These beating signals exhibit one of the main characteristics of stable asynchronous mode-locking. They indicate the slow periodic timing position modulation of the pulses caused by asynchronous modulation.

3.5 Discussion and Summary

We have also compared the behavior of our laser when operated with synchronous modulation. We find the asynchronous mode-locking shows superior performance than the synchronous mode-locking in two aspects. The first one is the higher SMSR which leads to more stable operation. The reason why the asynchronous mode-locking can achieve high SMSR is because the slow periodic timing position modulation of

the pulses caused by asynchronous modulation will also produce the slow periodic center-wavelength modulation of the pulses through the asynchronous phase modulation. The combination of the periodic center-wavelength drifting and the fixed filter can produce the equivalent sliding filter guiding-center soliton effects that have been extensively studied in soliton transmission. The combination of the periodic carrier frequency drift and the fixed optical filter in turns produces the equivalent sliding filter guiding-center soliton effects, with the difference that the optical filter is now fixed while the carrier frequency of the soliton is sliding. The solitons can survive with the presence of the sliding filtering effects due to their nonlinear-optic properties, while the noises will be filtered out due to their linear-optic properties. In this way, the supermode noises with asynchronous mode-locking can be lower than those with synchronous mode-locking. Another advantageous aspect of asynchronous mode-locking is that the pulse width is much shorter than that in synchronous mode-locking, since the pulse width of soliton is determined by the laser cavity parameters instead of the phase modulator. When the modulation frequency is exactly equal to the cavity harmonic frequency, the optical bandwidth is reduced to 0.5 nm and we can no longer observe sub-ps pulses.

The above mentioned results prove the advantages of the asynchronous modulation scheme. We believe the superior performance of our mode-locked fiber laser is due to the combination of APM, SPM with filtering, and asynchronous mode locking in a single fiber laser cavity. In addition, the effect additive-pulse limiting (APL) should also be helpful in stabilizing the laser [3,22]. By adjusting the bias point of additive-pulse interference through the adjustment of the two polarization controllers, either APM or APL or a combination of both effects can be achieved [3,22,23]. The APL effect will help to reduce the laser noises. Such a noise suppression effect is sensitive to the adjustment of the two polarization controllers. This is one of the

characteristics that indicate the presence of the APL effect. Even though all these mechanisms are included in the laser operation simultaneously, the structure of our hybrid mode-locked fiber laser is still rather simple.

We have found that the average cavity dispersion and the pump power are very crucial to the operation of asynchronous mode-locking. If the average cavity dispersion is unchanged, when the pulse repetition rate increases, the pump power should also be increased to keep the pulse energy close to that at the lower repetition rate. In this way the nonlinear effects in the laser cavity can be kept strong enough to support the stable operation of the mode-locked fiber laser at a higher repetition rate. One can estimate the soliton energy by the soliton area theorem. Given the fact that the average cavity dispersion parameter β_2 is $-2.26 \text{ ps}^2/\text{km}$, the nonlinear coefficient γ is $1.7 \text{ (km} \cdot \text{W)}^{-1}$, and the pulsewidth is 816 fs, the soliton energy inside the cavity is estimated to be 3.14 pJ, which is consistent with the pulse energy we observed experimentally.

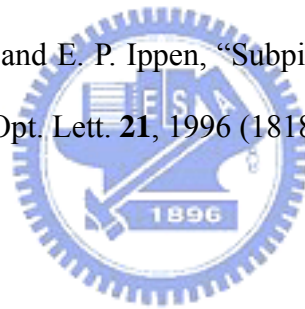
To summarize, we have successfully demonstrated a 10 GHz femtosecond mode-locked Er-fiber soliton laser achieved by asynchronous phase modulation. The output of the laser exhibits unique and interesting characteristics of slow periodic timing-position and center-wavelength sweep, which may have the potential for developing interesting new applications. The slowly varying timing position should not cause problems for optical transmission applications since the synchronization circuit of the receiver can follow it. However, the optical-carrier-frequency sweep may make the laser not suitable for frequency metrology applications. On the other hand, the periodic variation of the timing position may find some new uses in optical sampling applications, in which the timing-sweep of the sampling pulses can be automatically achieved. In the future more investigation can be pursued along this direction.

References for Chapter 3:

- [1] M. Nakazawa, H. Kubota, K. Suzuki, E. Yamada, and A. Sahara, "Ultra-high speed and long-distance TDM and WDM soliton transmission technology," *IEEE J. Selected Topics Quantum Electron.* **6**, 363 (2000).
- [2] S. Watanabe, R. Okabe, F. Futami, R. Hainberger, C. Schmidt-Langhorst, C. Schubert, H. G. Weber, "Novel fiber Kerr-switch with parametric gain: demonstration of optical demultiplexing and sampling up to 640 Gb/s," in *Proceedings of European Conference on Optical Communication (Stockholm, Sweden, 2004)*, Th4.1.6.
- [3] C. X. Yu, H.A. Haus, and E.P. Ippen, "Gigahertz-repetition-rate mode-locked fiber laser for continuum generation," *Opt. Lett.* **25**, 1418 (2000).
- [4] F. Ö Ilday, J. Chen, and F. X. Kärtner, "Generation of sub-100fs pulses at up to 200 MHz repetition rate from a passively mode-locked Yb-doped fiber laser," *Opt. Express* **13**, 2716 (2005).
- [5] C. X. Yu, H. A. Haus, and E. P. Ippen, "Soliton squeezing at gigahertz rate in Sagnac loop," *Opt. Lett.* **26**, 669 (2001).
- [6] M. E. Grein, L. A. Jiang, H. A. Haus, E. P. Ippen, C. McNeilage, J. H. Searls, R. S. Windeler, "Observation of quantum-limited timing jitter in an active, harmonically mode-locked fiber laser," *Opt. Lett.* **27**, 957 (2002).
- [7] T. F. Carruthers and I. N. Duling III, "10GHz, 1.3-ps erbium fiber laser employing soliton pulse shortening," *Opt. Lett.* **21**, 1927 (1996).
- [8] E. Yoshida, Y. Kimura, and M. Nakazawa, "20GHz, 1.8ps pulse generation from a regeneratively mode-locked erbium-doped fiber laser and its femtosecond pulse compression," *Electron. Lett.* **31**, 377, (1995).
- [9] M. Nakazawa, and E. Yoshida, "A 40GHz 850-fs regeneratively FM mode-locked

- polarization-maintaining erbium fiber ring laser,” *IEEE Photon. Technol. Lett.* **12**, 1613 (2000).
- [10] M. Margalit, C. X. Yu, S. Namiki, E. P. Ippen, and H. A. Haus, “Harmonic mode locking using regenerative phase modulation,” *IEEE Photon. Technol. Lett.* **10**, 337 (1998).
- [11] C. R. Doerr, H. A. Haus, and E. P. Ippen, “Asynchronous soliton mode locking,” *Opt. Lett.* **19**, 1958 (1994).
- [12] H. A. Haus, D. J. Jones, E. P. Ippen, and W. S. Wong, “Theory of soliton stability in asynchronous modelocking,” *IEEE J. Lightwave Technology* **14**, 622 (1996).
- [13] M.-F. Tie, W.-W. Hsiang and Y. Lai, “A femtosecond hybrid mode-locked Er-fiber soliton laser by asynchronous phase modulation,” in *Proceedings of Pacific Rim Conference on Lasers and Electro-Optics*(Taipei, Taiwan, 2003), Vol. 1, 34.
- [14] W.-W. Hsiang, C.-Y. Lin, M.-F. Tien, and Y. Lai, “Direct generation of 10 GHz 816 fs pulse train from an erbium-fiber soliton laser with asynchronous phase modulation,” *Opt. Lett.* **30**, 2493 (2005).
- [15] D. Kuizenga and A. E. Siegman, “FM and AM Mode Locking of Homogeneous Laser—Part I: Theory,” *IEEE J. Quantum Electron.* **6**, 694 (1970).
- [16] D. Kuizenga and A. E. Siegman, “FM and AM Mode Locking of Homogeneous Laser—Part II: Experimental results in a Nd-YAG Laser With Internal FM Modulator,” *IEEE J. Quantum Electron.* **6**, 709 (1970).
- [17] L. F. Mollenauer, J. P. Gordon, and S. G. Evangelides, ”The sliding-frequency guiding filter: an improved form of soliton jitter control,” *Opt. Lett.* **17**, 1575 (1992).
- [18] S. Burtsev and D. J. Kaup, “Effective control of a soliton by sliding-frequency

- guiding filters,” J. Opt. Soc. Am. B **14**, 627 (1997)
- [19] H. A. Haus and A. Mecozzi, “Noise of Mode-Locked Lasers,” IEEE J. Quantum Electron. **29**,983 (1993).
- [20] G. T. Harvey and L. F. Mollenauer, “Harmonically mode-locked fiber ring laser with an internal Fabry-Perot stabilizer for soliton transmission,” Opt. Lett. **18**, 107 (1993).
- [21] M. Nakazawa, K. Tamura, and E. Yoshida, “Supermode noise suppression in a harmonically modelocked fiber laser by self phase modulation and spectral filtering,” Electron. Lett. **32**, 461 (1996).
- [22] C. R. Doerr, H. A. Haus, E. P. Ippen, M. Shirasaki, and K. Tamura, “Additive pulse limiting,” Opt. Lett. **19**, 31 (1994).
- [23] D. J. Jones, H. A. Haus, and E. P. Ippen, “Subpicosecond solitons in an actively mode-locked fiber laser,” Opt. Lett. **21**, 1996 (1818).



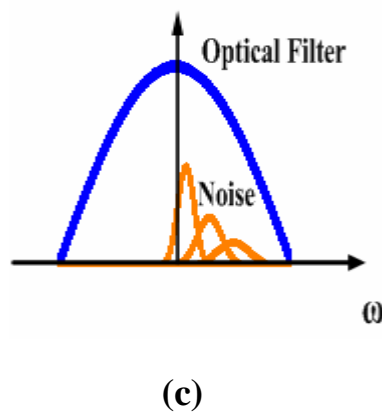
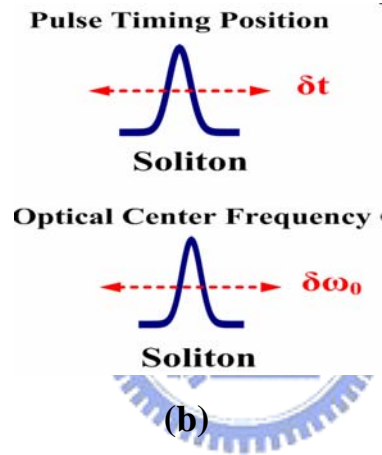
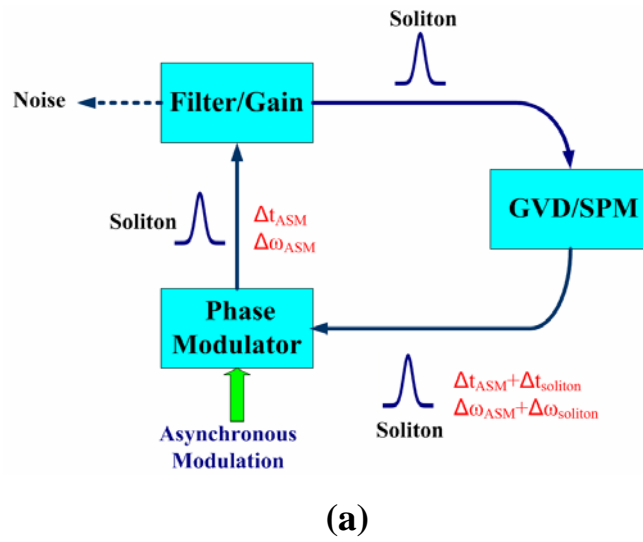


Fig. 3-1 (a) Laser cavity with the gain, the filter, GVD, SPM and the phase modulation driven asynchronously (b) Slow modulation in asynchronous soliton mode-locking (c) Noise clean-up effect in asynchronous soliton mode-locking.

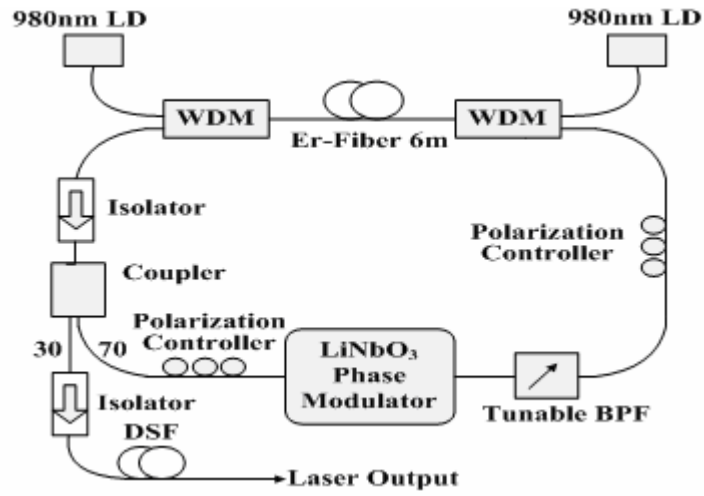


Fig. 3-2 Schematic of the asynchronously mode-locked Er-fiber laser.

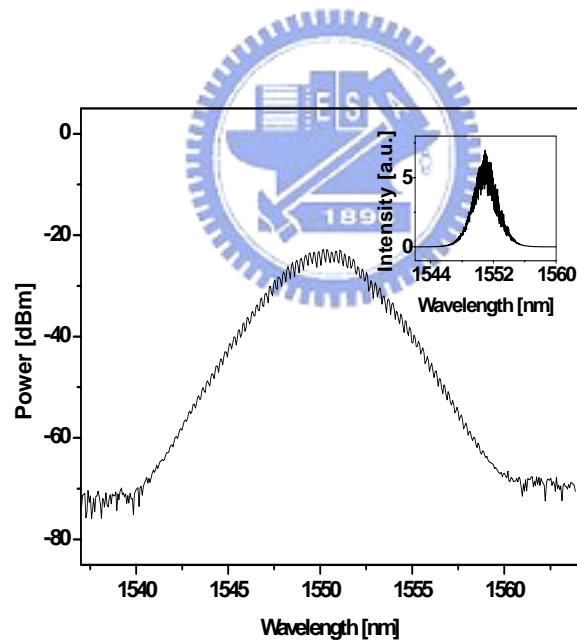


Fig. 3-3 (a)

Fig. 3-3 Optical characteristics of the pulse train from asynchronous mode-locking: (a) the optical spectrum with measurement resolution=0.07nm (inset: on a linear scale).

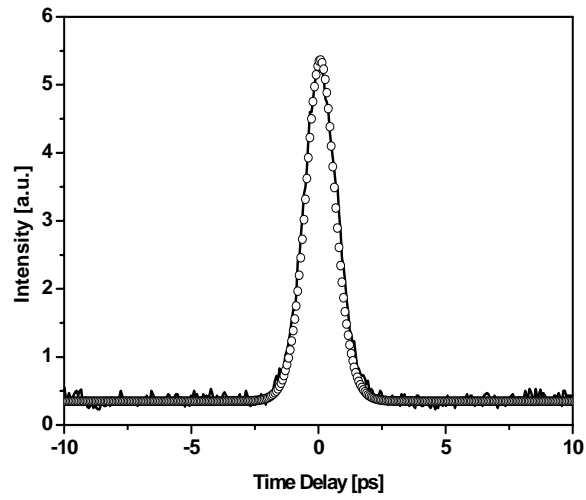


Fig. 3-3(b)

Fig. 3-3(b) Optical characteristics of the pulse train from asynchronous mode-locking: (b) the autocorrelation trace (the solid curve) and the fitting curve (the empty circles) assuming sech^2 pulse shape.

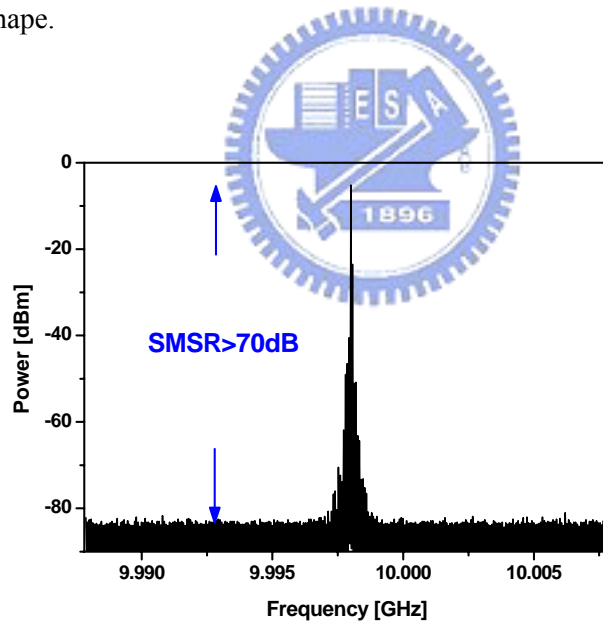


Fig. 3-4 (a)

Fig. 3-4(a) RF spectra of the pulse train from asynchronous mode-locking: (a) 20 MHz span, SMSR > 70 dB.

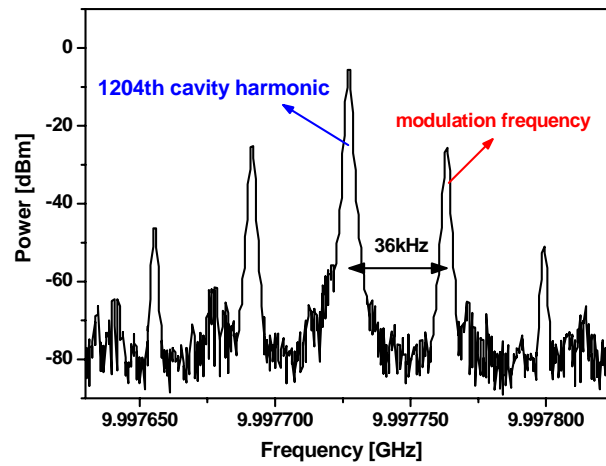


Fig. 3-4(b)

Fig. 3-4(b) RF spectra of the pulse train from asynchronous mode-locking: (b) 200 kHz span, detuning frequency = 36 kHz.



Chapter 4

Long-Term Stabilization of Asynchronously Mode-Locked Er-Fiber Soliton Laser

4.1 Introduction

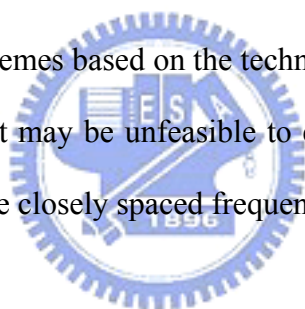
Over the past decades, a lot of research efforts have been devoted to develop mode-locked fiber laser sources that can meet the specific requirements for various applications. Among these works, one of the most challenging parts is to generate ultrashort pulses at high repetition rates directly from a mode-locked fiber laser [1-3]. In previous chapter, asynchronous soliton mode-locking has been demonstrated to be able to provide a good solution for this issue. Optical pulse trains of 816 fs at 10GHz with the supermode suppression ratio (SMSR) > 70 dB in the $1.55 \mu\text{m}$ wavelength can be directly obtained from the laser output, as long as the deviation frequency between the cavity harmonic frequency and the phase modulation frequency is kept within the suitable range of 15–40 kHz [4-6]. Such sub-ps pulses at 10 GHz or an even higher repetition rate should be very useful for applications in high-speed optical communication [7], ultrafast optical signal processing [8], and other scientific researches [3,9,10]. However, in order to utilize these asynchronously mode-locked Er-fiber soliton lasers in practical applications, the long-term stabilization issues need to be considered first. Because of the long cavity length, mode-locked fiber lasers are unavoidably sensitive to environmental fluctuations due to temperature variation as well as vibration [11,12]. These environmental changes will lead to a drift in the cavity harmonic frequency and thus destroy the stable operation of mode-locking in the long run.

In the literature, several methods based on the techniques of RF phase locking have been successfully developed to long-term stabilize the typical mode-locked fiber lasers with synchronously active modulation [1,13]. However, these schemes can not be directly applied to the asynchronously mode-locked lasers because their harmonic frequencies of the laser output are accompanied with closely spaced frequency sidebands resulted from the slow modulation of pulse timing position due to asynchronous mode-locking. This will cause some difficulty in the schemes of RF phase locking to cleanly obtain the cavity harmonic frequency. Therefore a new stabilization scheme is needed to be developed for asynchronously mode-locked fiber lasers.

In this chapter, we propose and successfully demonstrate a new stabilization scheme for a 10 GHz 0.8 ps asynchronously mode-locked Er-fiber soliton laser. It is based on controlling the cavity length to lock the deviation frequency at a suitable value, i.e., 25 kHz. Rather than using high-speed RF electronics to extract the 10 GHz cavity harmonic frequency, simple and low-frequency feedback electronics is enough to directly measure the shift of the deviation frequency. This can be achieved because the frequency sidebands due to asynchronous modulation will also appear in the output electronic frequency spectrum close to DC. The present method thus offers us an economic and simple approach with the same advantages as in Ref [14], in which the low-speed electronics of several tens of kHz in the feedback control loop is enough to stabilize mode-locked fiber lasers with the pulse repetition rate higher than 10 GHz. Details of the experimental setup and the achieved results for the proposed stabilization scheme will be presented in the following sections.

4.2 Frequency Sidebands of Laser Output

The slow periodic modulation in the pulse timing position is one of the main characteristics of asynchronous mode-locking and can be observed experimentally from the RF spectrum of the laser output. Figure 4-1(b) shows the same RF spectrum as in Fig. 4-1(a), except with a smaller span of 500 kHz. The main cavity harmonic frequency is 10.005974 GHz, and the modulation frequency is 10.005999 GHz. The frequency difference δf between the main cavity harmonic frequency and the modulation frequency is 25 kHz. The slow 25 kHz modulation of the pulse timing position is the reason that causes the appearance of frequency sidebands in the RF spectrum. As shown in Fig. 4-1(b), the frequency components around 10 GHz compose a series of frequency sidebands with the spacing equal to the deviation frequency of 25 kHz. These frequency sidebands around 10 GHz should cause some difficulty in the long-term stabilization schemes based on the technique of RF phase-locking, since in the feedback control loop it may be unfeasible to extract the 10 GHz main cavity harmonic frequency from these closely spaced frequency components[1,13].



4.3 Deviation-Frequency Extraction

Such frequency sidebands will also exist at other multiples of the pulse repetition rate. Most importantly, similar frequency sidebands can also be observed near DC. As shown in Fig. 4-2(a), three sideband peaks at multiple deviation frequencies (δf , $2 \times \delta f$, and $3 \times \delta f$) can be clearly observed. The frequency sidebands near DC provide us a simple approach to obtain the deviation frequency shift by using only low-frequency electronics. As shown in Fig. 4-2(b), a sharp cutoff (135dB/Octave) low-pass filter [15] and an amplifier can remove all the sideband peaks except for the first frequency peak closest to DC. The measured electronic spectrum after the low-pass filter and the amplifier is shown in Fig. 4-2(c), in which the deviation frequency peak around 25

kHz can be clearly seen. It can be used as a good error signal required in the feedback control loop for stabilizing the fiber laser, since the shift of the cavity harmonic frequency due to environmental fluctuations will also directly cause the shift of the deviation frequency.

4.4 Long-Term Stabilization Based on Deviation-Frequency Locking

In order to achieve the long-term stabilization of asynchronous mode-locked Er-fiber soliton lasers successfully, both mechanisms of asynchronous mode-locking and hybrid mode-locking should be maintained during the stabilization operation [6]. The former mechanism relies on maintaining a suitable deviation frequency of 15–40 kHz between the modulation frequency and the cavity harmonic frequency. For the latter mechanism, the optical polarization evolution along the laser cavity should not be perturbed by the cavity length control unit. In this way, polarization additive mode-locking and additive pulse limiting can continue to maintain the same effects of pulse formation and pulse energy equalization. To meet the first requirement of keeping a suitable deviation frequency, we feedback-control the cavity length by a PZT to lock the deviation frequency at a suitable frequency, i.e., 25 kHz. As to the second requirement, since we do not observe obvious polarization changes when the cavity length is detuned by the PZT, it is automatically satisfied. The shift of the deviation frequency can be obtained by using a low-pass filter to extract the first peak closest to DC from the frequency sidebands near DC.

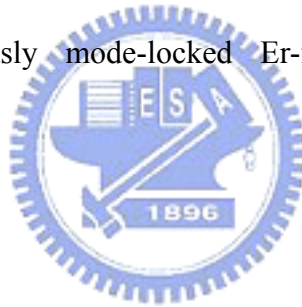
Our actual experiment to demonstrate long-term stabilization is described as follows. The asynchronously mode-locked fiber laser is fixed on the aluminum plate with a temperature controller to reduce the environmental temperature change. A PZT wound with the single-mode fiber is put in the laser cavity to adjust the cavity length.

As shown in Fig. 4-3, the feedback control loop composes a sharp cutoff (135dB/Octave) low-pass filter, an amplifier, a frequency counter, a computer, and a high voltage amplifier to drive the PZT. A small fraction of the laser output is detected by the photodiode. The low-pass filter can remove all the sideband peaks except for the first frequency peak closest to DC. The frequency counter (Agilent 53181A) can measure the deviation frequency and sends its digital output to the computer. The computer will then process the signal with suitable signal processing methods and then send the frequency error signal to the PZT driver to lock the deviation frequency at 25 kHz. The maximum amount of the frequency shift that can be produced by our PZT unit is about ± 25 kHz, which seems to be enough for long-term stabilization as long as the environmental temperature fluctuations are reduced to be small enough by the temperature controller. When the fiber laser is operating without the stabilization scheme, the typical deviation frequency is about ± 4 kHz in 7 minutes as shown in Fig. 4-4. Experimentally, a deviation frequency shift larger than 10 kHz will severely affect the stability of asynchronous mode-locking. Long-term stable operation is achieved when the stabilization scheme is turned on, as is shown in Fig. 4-4. The deviation frequency shift can be controlled to be within ± 300 Hz, limited by our frequency counter unit. Figure 4-5 shows the stabilized 10 GHz pulse train measured from a fast sampling oscilloscope.

The main advantage of this stabilization scheme is that it provides a simple and economic approach to stabilize asynchronously mode-locked fiber lasers. The high-speed electronics are not required in the feedback control loop and it is much easier to deal with the electronics in the kHz range. Furthermore, the same feedback control unit is suitable for even higher modulation frequencies. This is because the suitable deviation frequency always remains within the range of 15–40 kHz, despite the change of the pulse repetition rate.

4.5 Summary

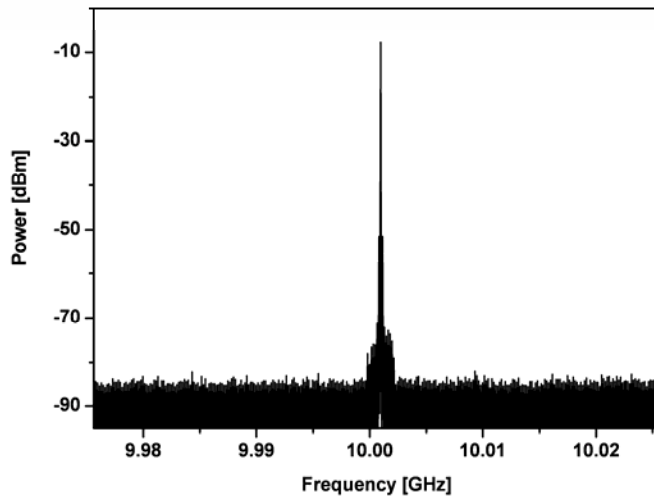
To summarize, without using high speed RF feedback electronics, the long-term stabilization of a 10 GHz 0.8 ps asynchronously mode-locked Er-fiber soliton laser has been proposed and demonstrated for the first time by controlling the cavity length to lock the deviation frequency at 25 kHz. The stabilization scheme is simple and economic, since only electronics in the kHz range are required for long-term stabilizing the mode-locked fiber laser with a 10 GHz repetition rate. Moreover, the same low frequency feedback control unit is suitable for other modulation frequencies, even when the pulse repetition rate is raised up to 40 GHz or more. Based on this stabilization scheme, stable sub-ps pulses with high repetition rates can be stably obtained from asynchronously mode-locked Er-fiber soliton lasers for real applications



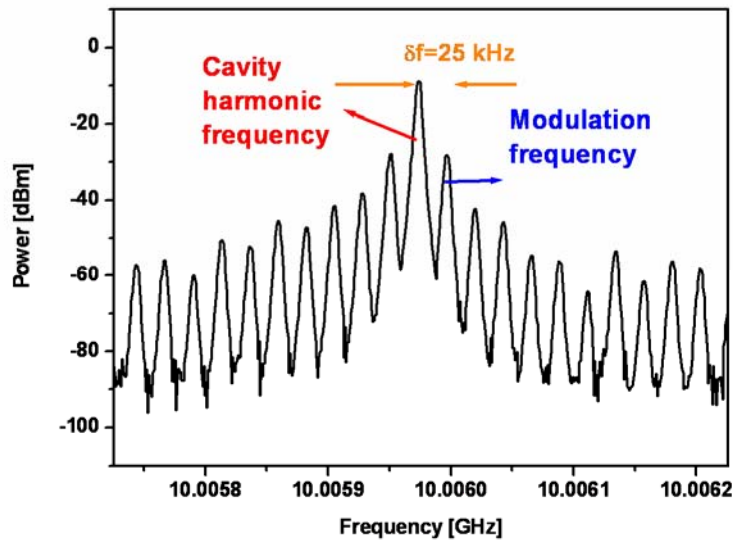
References for Chapter 4:

- [1] M. Nakazawa and E. Yoshida, "A 40-GHz 850-fs regeneratively FM mode-locked polarization-maintaining erbium fiber ring laser," *IEEE Photon. Technol. Lett.* **12**, 1613-1615 (2000).
- [2] E. Yoshida, Y. Kimura, and M. Nakazawa, "20GHz, 1.8ps pulse generation from a regeneratively modelocked erbium-doped fiber laser and its femtosecond pulse compression", *Electron. Lett.* **31**, 377-378 (1995).
- [3] C. X. Yu, H. A. Haus, E. P. Ippen, W. S. Wong, and A. Sysoliatin, "Gigahertz-repetition-rate mode-locked fiber laser for continuum generation," *Opt. Lett.* **25**, 1418-1420 (2000).
- [4] C. R. Doerr, H. A. Haus, and E. P. Ippen, "Asynchronous soliton mode locking," *Opt. Lett.* **19**, 1958-1960 (1994).
- [5] H. A. Haus, D. J. Jones, E. P. Ippen, and W. S. Wong, "Theory of soliton stability in asynchronous modelocking," *J. Lightwave Technol.* **14**, 622-627 (1996).
- [6] W.-W Hsiang, C.-Y Lin, M.-F Tien, and Y. Lai, "Direct generation of a 10 GHz 816 fs pulse train from an erbium-fiber soliton laser with asynchronous phase modulation," *Opt. Lett.* **30**, 2493-2495 (2005).
- [7] M. Nakazawa, H. Kubota, K. Suzuki, E. Yamada, and A. Sahara, "Ultrahigh-speed long-distance TDM and WDM soliton transmission technologies", *IEEE J. Selected Topics Quantum Electron.* **6**, 363-396 (2000).
- [8] S. Watanabe, R. Okabe, F. Futami, R. Hainberger, C. Schmidt-Langhorst, C. Schubert, H. G. Weber, "Novel fiber Kerr-switch with parametric gain: demonstration of optical demultiplexing and sampling up to 640 Gb/s", in *Proceedings of European Conference on Optical Communication (Stockholm, Sweden, 2004)*, Th4.1.6.

- [9] C. X. Yu, H. A. Haus, and E. P. Ippen, "Soliton squeezing at the gigahertz rate in a Sagnac loop," *Opt. Lett.* **26**, 669-671 (2001).
- [10] J. W. Nicholson, M. F. Yan, P. Wisk, J. Fleming, F. DiMarcello, E. Monberg, A. Yablon, C. Jørgensen, and T. Veng, "All-fiber, octave-spanning supercontinuum," *Opt. Lett.* **28**, 643 (2003).
- [11] M. Nakazawa, E. Yoshida, E. Yamada, and Y. Kimura, "A Repetition-Rate Stabilized and Tunable, Regeneratively Mode-Locked Fiber Laser Using an Offset-Locking Technique," *Jpn. J. Appl. Phys.* **35**, L 691 (1996).
- [12] L. E. Nelson, D. J. Jones, K. Tamura, H. A. Haus and E. P. Ippen, "Ultrashort-pulse fiber ring lasers," *Appl. Phys. B* **65**, 277 (1997).
- [13] X. Shan, D. Cleland and A. Ellis, "Stabilising Er fibre soliton laser with pulse phase locking," *Electron. Lett.* **28**, 182-184 (1992).
- [14] H. Takara, S. Kawanishi, and M. Saruwatari, "Stabilisation of a modelocked Er-doped fibre laser by suppressing the relaxation oscillation frequency component," *Electron. Lett.* **31**, 292-293 (1995).
- [15] <http://www.kemo.com/>.

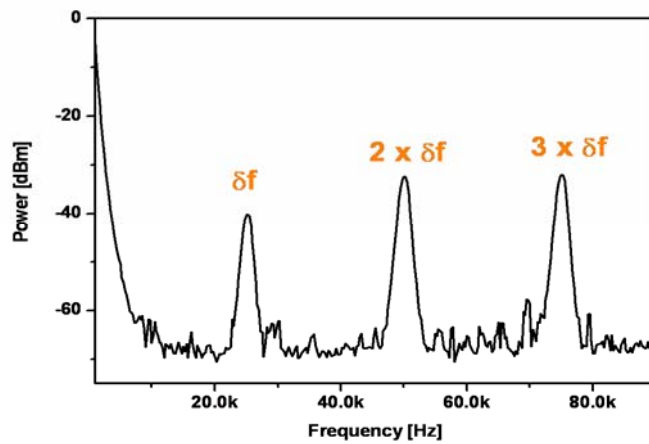


(a)

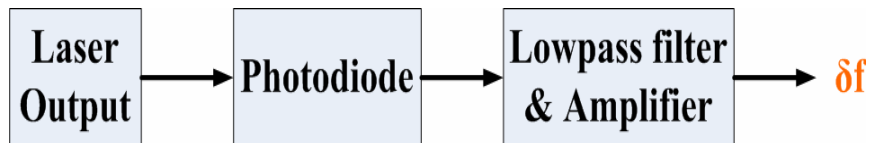


(b)

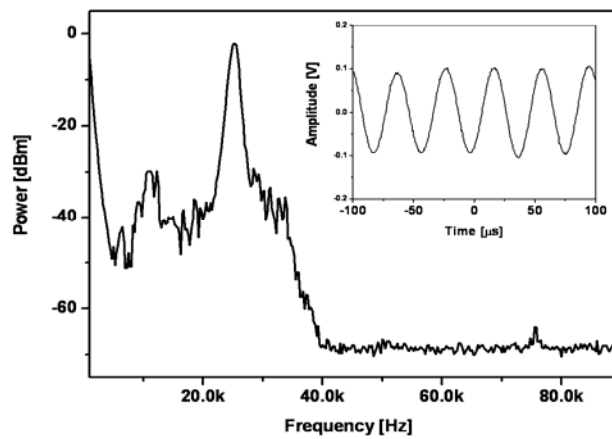
Fig. 4-1 RF spectra near 10 GHz. (a) Span of 50 MHz, SMSR > 70 dB (b) Span of 500 kHz, deviation frequency δf of 25 kHz.



(a)



(b)



(c)

Fig. 4-2 (a) Electronic frequency sidebands of laser output near DC (b) Electronics of deviation-frequency extraction (c) Electronic frequency spectrum after the lowpass filter (inset, signal in the time domain).

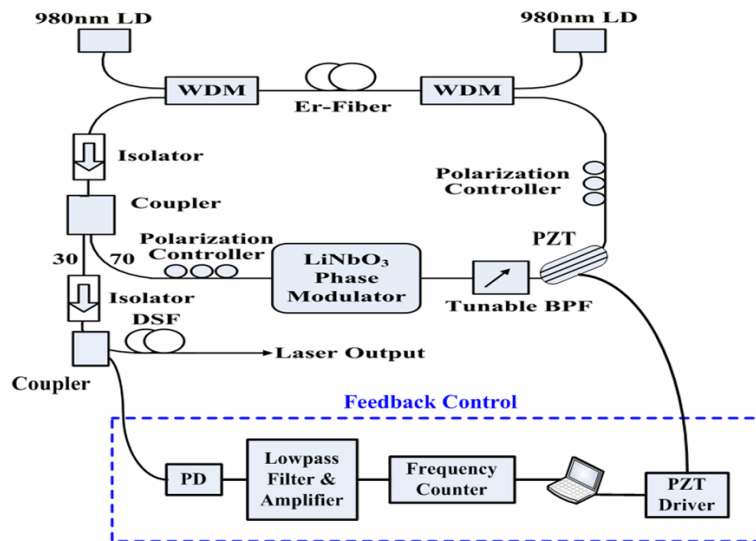


Fig. 4-3 Schematic of the mode-locked Er-fiber laser and the feedback control. BPF, band-pass filter; PD, photodiode; DSF, dispersion shift fiber.

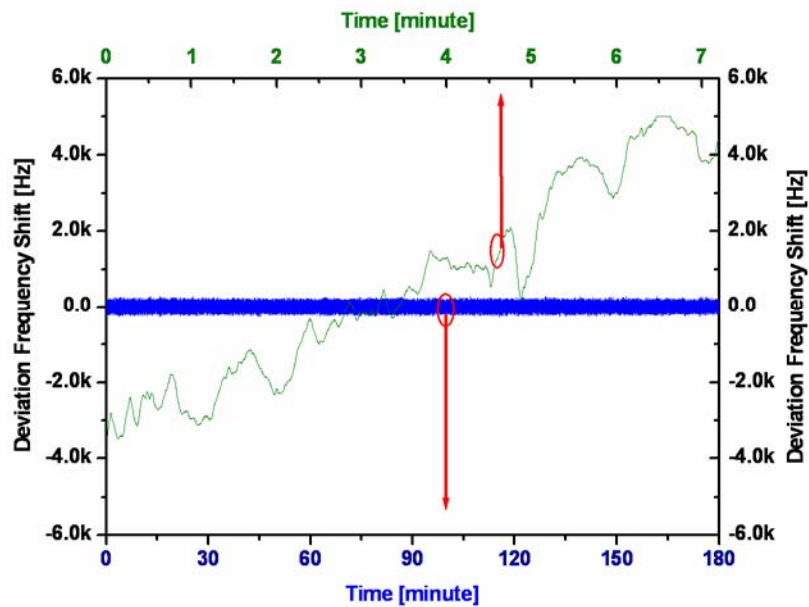


Fig. 4-4 Long-term stabilization and deviation frequency shift. Green curve: without the stabilization scheme, upper axis; blue curve: with the stabilization scheme, lower axis.

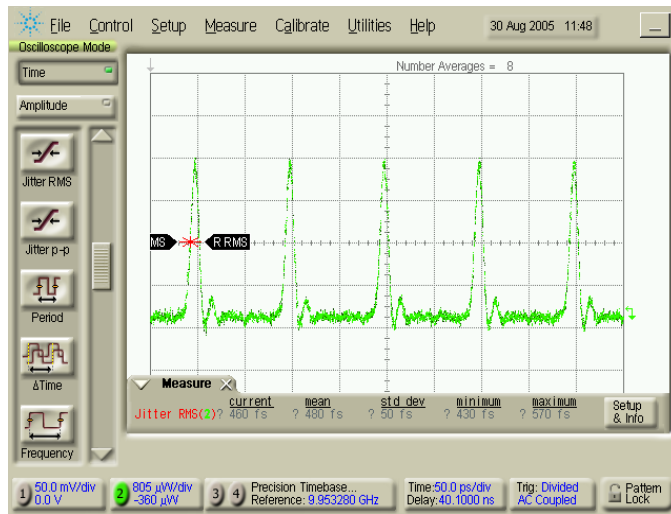


Fig. 4-5 10 GHz pulse train measured from a fast sampling oscilloscope.



Chapter 5

New Stable 10 GHz Bound Soliton Pairs

5.1 Introduction

Solitons in optical fibers are not only important for long link optical communication, but also are useful for building new types of mode-locked fiber lasers. Actually the mode-locked fiber laser has become a platform for demonstrating new types of soliton phenomena, including the formation of bound soliton states. In the literature, various kinds of soliton bound states have been experimentally observed in passively mode-locked fiber lasers [1-4]. These experimental results can provide useful information for investigating the underlying nonlinear soliton dynamics. Depending on the formation mechanism (i.e., short-range or long-range soliton interactions), bound soliton states can be divided into two main categories [4]. Some of the reported passively mode-locked fiber lasers with equivalent fast saturable absorbers belong to the first category of short-range soliton interaction. They are typically modeled by the complex Ginzburg-Landau equation, which has been shown to exhibit bound soliton solutions within certain parameter regimes [5,6]. On the contrary, for the second category of long-range soliton interaction, the tails of the adjacent solitons do not overlap and thus direct soliton interaction can be ignored. In some of the reported cases the dispersive waves resulted from the periodic perturbations in the laser cavity have been shown to have major influence on the stabilization of these bound soliton states with large time separation [1,4]. Generally speaking, the soliton bound states in passively mode-locked fiber lasers are found to have fixed relative phase differences and fixed (even quantized) time separations [1]. They are also found to exhibit

superior stability when compared to the single pulse cases [3].

The schematic diagrams of bound solitons in mode-locked fiber lasers are drawn in Fig. 5-1. Figure 5-1(a) shows the one single bound soliton pair circulating in the passively mode-locked fiber laser. Therefore the repetition rate of bound soliton pair is equivalent to cavity frequency. Up to now, most of the soliton bound states reported in the literature in passively mode-locked fiber laser are at fundamental repetition rate as shown in Fig. 5-1(a). Figure 5-1(b) shows the bound soliton fiber laser at cavity harmonic repetition rate in the mode-locked fiber laser. This means that there are N (more than one) soliton pairs simultaneously circulating in the fiber laser cavity. In contrast to passive mode-locking, so far there is no report on the observation of stable bound soliton states at cavity harmonic repetition rate in any active/hybrid mode-locked lasers.

In this chapter we experimentally demonstrate the existence of stable new bound soliton pairs at the 10 GHz repetition rate in a hybrid FM harmonic mode-locked Er-fiber laser, in which there are 1177 soliton pairs simultaneously circulating in the laser cavity [7]. The details of this hybrid FM harmonic mode-locked Er-fiber laser are described in Section 5-2. The 10 GHz bound soliton pairs are observed when the laser harmonic frequency is locked exactly at the modulation frequency. In Section 5-3, the experimental observations of these bound soliton pairs are shown, including the intensity SHG autocorrelation trace, the optical spectrum, the RF spectrum of the laser output, and the pulse train from the fast sampling scope. These data shows that the two solitons in the soliton pair have the identical pulse shape and are with the anti-phase (π phase difference). Their time separation is about three times the FWHM soliton-width of the individual solution. Based on these observed results, in Section 5-4, the corresponding mechanisms for explaining the formation as well as the superior stability of these closely bound soliton pairs are given. This theoretical model

is examined by soliton perturbation theory and shows that the time separation between the bound soliton pair is dependent on the modulator strength of the phase modulator. The dependence of the time separation between the bound soliton pair on the modulator strength is directly observed experimentally and consistent with our theoretical prediction. Finally, a brief summary of this chapter is given.

5.2 10 GHz Hybrid FM Mode-Locked Er-Fiber Laser

Figure 5-2 shows our mode-locked Er-fiber laser with the feedback control of the cavity length. The configuration of the fiber laser cavity is basically the same as in Ref [7,8] and thus the detailed cavity parameters can be found there. The main difference between our laser configuration and typical actively mode-locked fiber laser configuration is that a phase modulator with enough polarization dependent loss and two polarization controllers are used. By employing the third order nonlinearity of the optical fibers, the effects of polarization additive pulse mode locking (APM) or additive pulse limiting (APL) can be implemented to achieve shorter pulse width or better stability [7-9]. Depending on the driving RF signal for the phase modulator and the states of the polarization controllers, a variety of mode-locking regimes can be obtained, including the passive mode-locking and synchronously/asynchronously active/hybrid mode-locking [7,8]. Bound soliton pairs are observed in the regime of synchronously harmonic mode-locking at 10 GHz. They can remain stable as long as the cavity length is locked with enough accuracy. In order to achieve long-term stability, the fiber laser is fixed on an aluminum plate with the temperature controller to reduce the temperature variation. A PZT wounded with the single mode fiber is also put into the laser cavity to feedback-control the cavity length based on the technique

of RF phase locking [10]. The phase differences between optical pulses and the modulator's driving signals are compared in the RF mixer. And then, according to the phase differences, the proportional and integral (PI) controller will generate the error signals to drive the PZT. The fundamental cavity harmonic frequency is 8.5 MHz, implying there are 1177 pulses simultaneously circulating inside the cavity when the pulse repetition rate is 10 GHz.


5.3 Experimental Observations of 10 GHz Bound Soliton Pairs

Figure 5-3 shows the SHG autocorrelation trace of the soliton bound state, which clearly indicates the existence of two pulses. From the plot one can infer that the two pulses are almost identical and the FWHM of the pulse width is 1.3 ps. The time separation between the two pulses is only about three times the individual pulse width, i.e., 4 ps. Such small separation suggests that there should be an attractive or repulsive force exerted on the respective soliton due to direct soliton interaction. The sign of the force (attractive or repulsive) will depend on the phase difference between the two solitons [11].

The solid curve in Fig. 5-4 shows the optical spectrum of the bound solitons. The optical spectrum is periodically modulated, which results from the interference between the two solitons. The dots in Fig. 5-4 show the fitting of the interference in the optical spectrum with the assumption of two identical but time-shifted pulses. The parameters used in the fitting include the interference period of 1.95 nm and the soliton's optical FWHM bandwidth of 1.94 nm. The observed interference period in the optical spectrum is consistent with the pulse separation measured from the SHG autocorrelation. The time-bandwidth product of the individual pulse is 0.32, indicating that the pulse is with a sech pulse-shape and with little chirp. Since in

Fig.5-3 the central interference dip is in the center of the optical power spectrum, it indicates that the phase difference of the two solitons is equal to π . The superior stability is also one of the noticeable characteristics when the laser is working in the bound state regime. As shown in Fig. 5-5, when the cavity length is kept locked, the supermode suppression ratio (SMSR) is more than 70 dB. Figure 5-6 shows the 10 GHz bound soliton pairs measured from the fast sampling scope. The rising/fall time of the photodiode and electronic is not fast enough to observe the individual pulses. However, the equal heights of the measured pulse shapes indicate the 10 GHz bound soliton pairs are very stable and have a high SMSR, as same as the measurement result from the RF spectrum analyzer.

5.4 Theoretical Model of 10 GHz Bound Soliton Pairs



Conceptually the formation of stable bound soliton states can be described by the following two steps. First of all, similar to multiple pulse operation in passive mode-locking, pulse splitting can occur through the effect of soliton energy quantization, provided that the gain medium can support enough pulse energy [12]. In our laser, pulse splitting can also be triggered by adjusting the polarization controllers to modify the threshold of APM or APL. Secondly, to achieve stable bound soliton pairs, each split soliton should experience the balanced attractive and repulsive forces simultaneously when propagating along the laser cavity. In our case, because of the π phase difference and the relatively close separation, the two solitons should repel each other due to direct soliton interaction. However, as to be explained below, we believe an effective attractive force will be introduced by the phase modulator and the anomalous group velocity dispersion (GVD) of the cavity. In an actively FM mode-locked fiber laser with net anomalous GVD, the pulses should be formed in the

center of the up-chirped modulation cycle [13]. This should be also true for the bound soliton case, as shown in Fig. 5-7. Under such situation, the front soliton will experience a negative frequency shift through the modulator, which leads to the decreasing of its group velocity through the anomalous GVD of the cavity. On the contrary, the back soliton will experience the increasing of the group velocity. Therefore the phase modulator and the anomalous GVD can provide the necessary equivalent attractive force to balance the repulsive force from direct soliton interaction.

The above description can be further examined quantitatively by a simple soliton perturbation theory [14], in which the evolution equations of the soliton parameters, including amplitudes $a_i(z)$, positions $s_i(z)$, frequencies $\omega_i(z)$ and phases $\theta_i(z)$, can be obtained during direct soliton interaction (without phase modulation). The bound soliton state is described by the sum of $u_i(z, t)$, where $u_i(z, t) = a_i(z)\text{Sech}[a_i(z)(t - s_i(z))]\exp[i\theta_i(z) - i\omega_i(z)t]$. With the identical pulse amplitude and the π phase difference, the sum and the difference of the soliton parameters of the two solitons remain unchanged, except for the position difference and frequency difference. They are described by

$$\frac{d\Delta s}{dz} = -\Delta\omega \quad (5.1)$$

$$\frac{d\Delta\omega}{dz} = -4a^3 \exp(-2\Delta s) \quad (5.2)$$

where $2a = a_1 + a_2$, $2\Delta\omega = \omega_1 - \omega_2$, and $2\Delta s = s_1 - s_2$. At steady state, since the time separation $2\Delta s$ is fixed at a constant value $2\Delta s_0$, the accumulated frequency difference during one cavity round trip can be estimated to be $-4a^3 \exp(-2\Delta s_0)z_c$ by Eq. (5.2), where z_c is the cavity length. In our experiment, the cavity length $z_c = 23.5$ m, average cavity GVD $\beta_2 = -5$ ps²/km, zero-order position difference

$2\Delta s_0 = 4$ ps and soliton's FWHM pulse width = 1.3 ps, the accumulated frequency difference during one cavity round trip is estimated to be $10.32 \text{ rad} \cdot \text{GHz}$. On the other hand, when the soliton pair passes through the up-chirped modulation cycle once, the two solitons obtain a relative frequency difference of $2M(2\pi f_M)^2 \Delta s_0$, where f_M is the modulation frequency (=10 GHz) and M is the modulation depth. Since the two induced frequency differences $-4a^3 \exp(-2\Delta s_0) z_c$ and $2M(2\pi f_M)^2 \Delta s_0$ should cancel each other at the steady state, we can infer that the modulation depth M is about 0.654 rad. This inferred value is in reasonable agreement with the estimated value from the driving RF power. The accumulated change of the position difference during one round trip will be zero when the accumulated frequency difference is equal to zero. Although the above simple theory does yield reasonable predictions agreed with experimental observations, we want to note that it should still be worthwhile to carry out theoretical studies based on a more complete laser model in the future.

The mechanism explained above suggests that the time separation should be dependent on the modulation depth M . We have experimentally verified this point and the results are shown in Fig. 5-8 and Fig. 5-9. Figure 5-8 shows measurement results of the SHG autocorrelations when the modulation depth is changed. As expected, the time separation decreases when the modulation depth is increased, which is also shown in Fig. 5-9. We believe this is a direct proof that the observed bound soliton state is a new soliton phenomenon which is fundamentally different from the previous reports in passively modelocked fiber lasers. Furthermore, the superior stability of the soliton bound state laser can also be explained within the same framework. Since the linear noises accompanied with the solitons will continuously experience the frequency shift by the phase modulator and will be eventually filtered out.

5.5 Summary

To summarize, for the first time, stable 10 GHz bound soliton pairs have been experimentally observed in a hybrid FM mode-locked Er-fiber laser. Their time separation is dependent on the modulation depth, indicating a new type of bound soliton phenomenon. We believe these closely adjacent soliton pairs are stably formed through the balance between the soliton direct interaction and the effective attracting force introduced by the phase modulation and the negative GVD of the cavity.

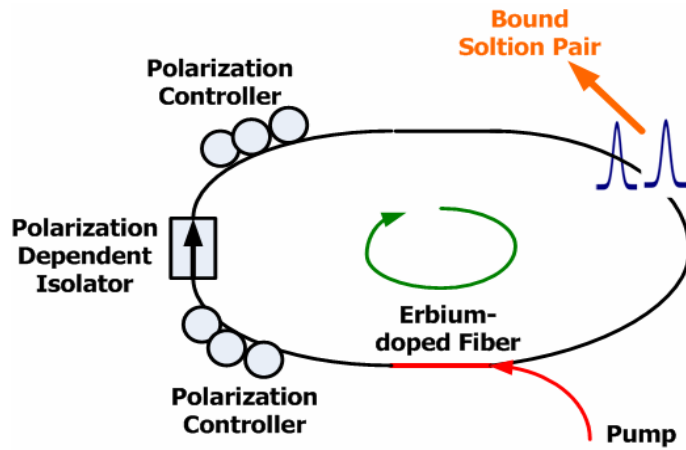


References for Chapter 5:

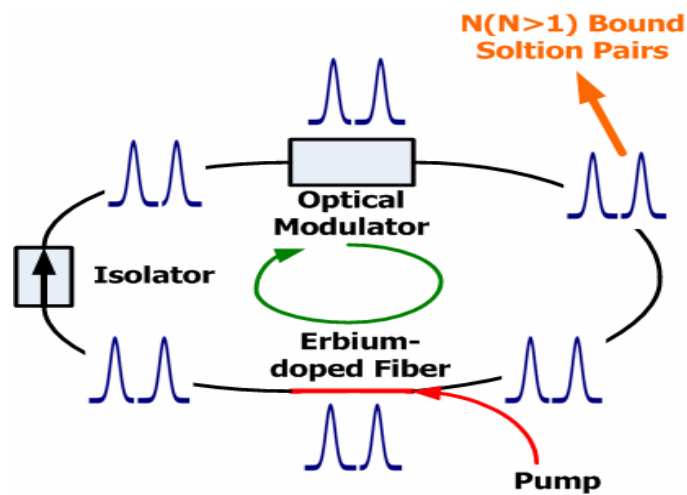
- [1] J. M. Soto-Crespo, N. Akhmediev, P. Grelu, and F. Belhache, “Quantized separations of phase-locked soliton pairs in fiber lasers,” *Opt. Lett.* **28**, 1757 (2003).
- [2] D. Y. Tang, W. S. Man, H. Y. Tam, and P. D. Drummond, “Observation of bound states of solitons in a passively mode-locked fiber laser,” *Phys. Rev. A* **64**, 033814 (2001).
- [3] F. Guty, P. Grelu, N. Huot, G. Vienne, and G. Millot, “Stabilisation of modelocking in fibre ring laser through pulse bunching,” *Electron. Lett.* **37**, 745 (2001).
- [4] D. Y. Tang, B. Zhao, L. M. Zhao, and H. Y. Tam, “Soliton interaction in a fiber ring laser,” *Phys. Rev. E* **72**, 016616 (2005).
- [5] B. A. Malomed, “Bound solitons in the nonlinear Schrödinger-Ginzburg-Landau equation,” *Phys. Rev. A* **44**, 6954 (1991).
- [6] N. N. Akhmediev, A. Ankiewicz, and J. M. Soto-Crespo, “Multisoliton Solutions of the Complex Ginzburg-Landau Equation,” *Phys. Rev. Lett.* **79**, 4047 (1997).
- [7] W.-W. Hsiang, C.-Y. Lin, and Y. Lai, “Stable new bound soliton in a 10 GHz hybrid frequency modulation mode-locked Er-fiber laser,” *Opt. Lett.* **31**, 1627 (2006).
- [8] W.-W. Hsiang, C.-Y. Lin, M.-F. Tien, and Y. Lai, “Direct generation of a 10 GHz 816 fs pulse train from an erbium-fiber soliton laser with asynchronous phase modulation,” *Opt. Lett.* **30**, 2493 (2005).
- [9] C. X. Yu, H. A. Haus, E. P. Ippen, W. S. Wong, and A. Sysoliatin, “Gigahertz-repetition-rate mode-locked fiber laser for continuum generation,” *Opt. Lett.* **25**, 1418 (2000).

- [10] X. Shan, D. Cleland, and A. Ellis, "Stabilising Er fibre soliton laser with pulse phase locking," *Electron. Lett.* **28**, 182 (1992).
- [11] J. P. Gordon, "Interaction forces among solitons in optical fibers," *Opt. Lett.* **8**, 596 (1983).
- [12] A. B. Grudinin, D. J. Richardson, and D. N. Payne, "Energy quantisation in figure eight fibre laser," *Electron. Lett.* **28**, 67 (1992).
- [13] K. Tamura and M. Nakazawa, "Pulse energy equalization in harmonically FM mode-locked lasers with slow gain," *Opt. Lett.* **21**, 1930 (1996).
- [14] T. Georges and F. Favre, "Modulation, filtering, and initial phase control of interacting solitons," *J. Opt. Soc. Am. B* **10**, 1880 (1993).





(a)



(b)

Fig. 5-1 Bound soliton pairs in mode-locked fiber laser. (a) Only one bound soliton pair circulates in the fiber laser cavity (the typical case in passively mode-locked fiber laser). (b) More than one ($N > 1$) bound soliton pairs circulate simultaneously in the fiber laser cavity (the case corresponding to the 10 GHz bound soliton pairs in our hybrid FM mode-locked Er-fiber laser).

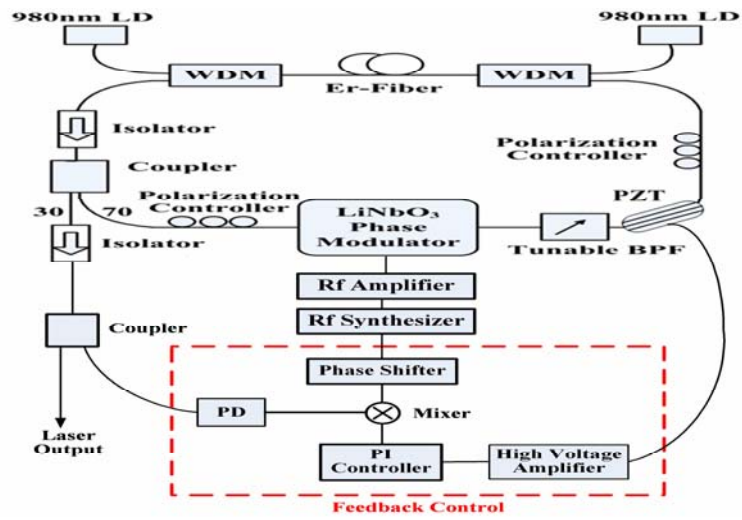


Fig. 5-2 Schematic of the mode-locked Er-fiber laser and the feedback control loop. PI, proportional and integral control module; PD, photodiode.

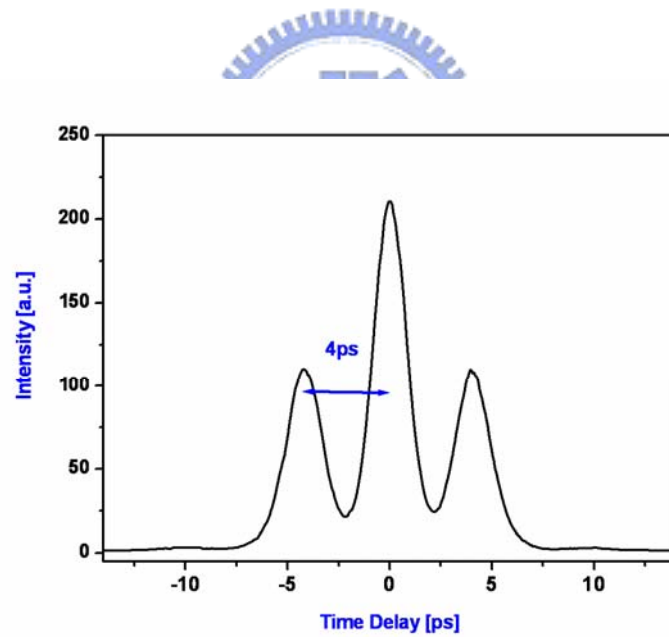


Fig. 5-3. SHG autocorrelation trace of the bound soliton pair.

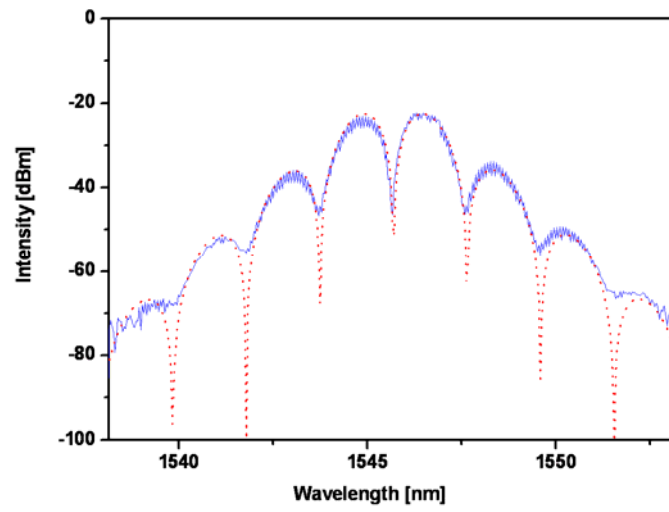


Fig. 5-4. Optical spectrum of the bound soliton pair (solid curve, measurement; dots, fitting).

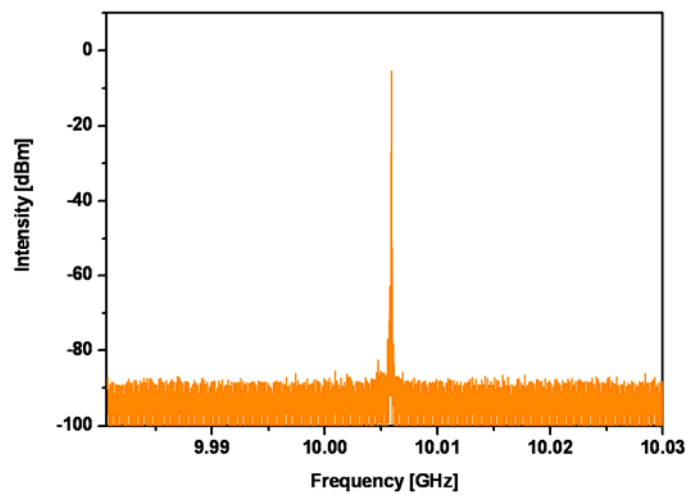


Fig. 5-5. RF spectrum of the 10 GHz bound soliton pair, SMSR > 70 dB.

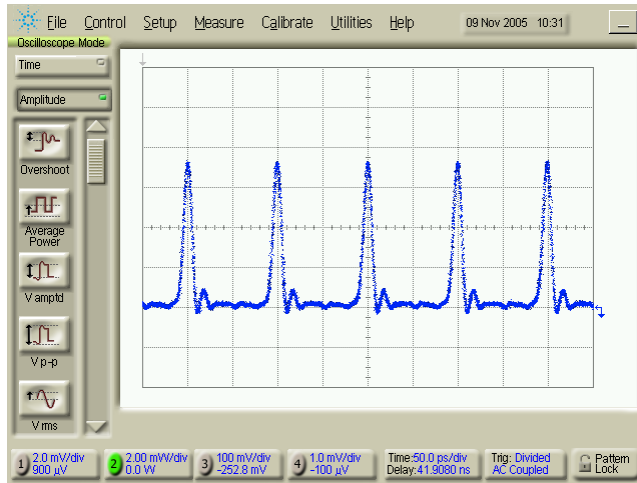


Fig. 5-6. Stable 10 GHz bound soliton pairs measured form the fast sampling scope.

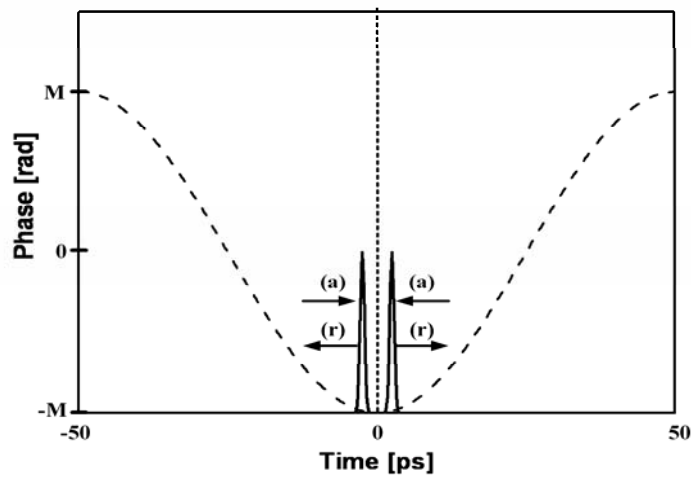


Fig. 5-7. Timing diagram between the phase modulation signal and the bound soliton pair. M : modulation depth.

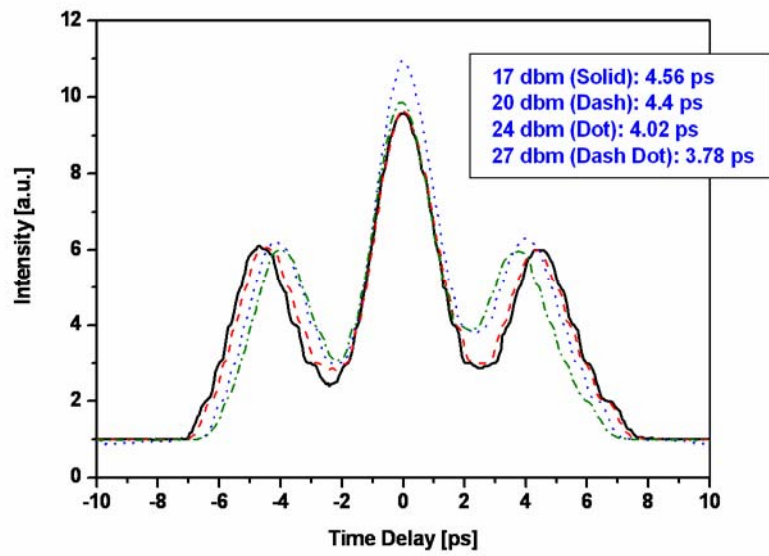


Fig. 5-8 Measurements of SHG autocorrelation traces when the driving RF power of the phase modulator varies.

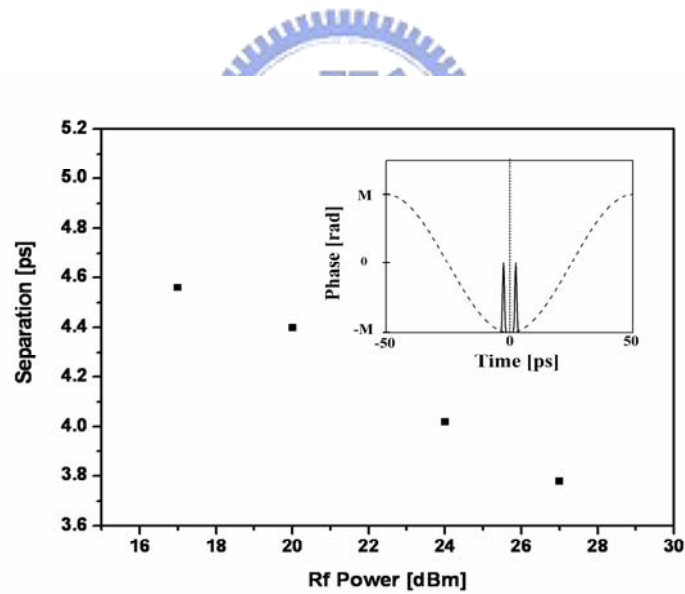


Fig. 5-9. Time separation versus the RF power of the phase modulator (inset, timing diagram between the phase modulation signal and the bound soliton pair. M, modulation depth).

Chapter 6

Conclusions and Future Work

6.1 Conclusions

In this thesis, a variety of soliton phenomena in Er-fiber lasers from passive mode-locking to active/hybrid mode-locking are investigated. Many similar soliton phenomena occur in long-distance soliton communication systems can be observed or can have their respective counterparts in mode-locked Er-fiber lasers. These include the perturbed solitons and dispersive waves, resonant instability and spectral sidebands, the noise clean-up effect of sliding-frequency guiding filters, soliton-continuum interaction, and soliton-soliton interaction. In addition to these well-known soliton phenomena, for the first time, a new type of stable bound soliton pairs in a 10 GHz hybrid FM Er-fiber laser is demonstrated and studied.

Investigation and understanding of these soliton effects are helpful for us to develop and implement new kinds of all-fiber mode-locked lasers which can not be achieved in typical mode-locking techniques. The efforts to look for effective solutions for combining passive and active mode-locking to achieve ultrashort pulse width and high repetition rate simultaneously, are presented in Section 2-4, Chapter 3, and Chapter 4. In Section 2-4, the passive harmonic mode-locking techniques based on soliton energy quantization have been demonstrated to be able to generate femtosecond pulses with the repetition rate up to 300 MHz. Although the spontaneous multiplication of repetition rate does not require any optical modulator or intracavity element inside the fiber laser, there still exists several disadvantages which may not be suitable for practical applications. The main limitation on the usage of

passive harmonic mode-locking is due to its low repetition rate, low SMSR, difficult tuning of the repetition rate, and poorer long-term stabilization.

In chapter 3 and chapter 4, we adopt the concept of sliding-frequency guiding center filter originally used in soliton communication to implement the asynchronously mode-locked (ASM) Er-fiber soliton laser, which can directly generate 0.8 ps 10 GHz SMSR > 70 dB pulses. The advantages of asynchronous soliton mode-locking are the ability to generate shorter pulse width and to suppress supermode noises. One of the main characteristics of this fiber soliton laser is the slow modulations of pulse timing position and pulse carrier frequency. In chapter 4, a long-term stabilization scheme for the asynchronously mode-locked Er-fiber soliton laser is proposed and demonstrated. Without using high-speed RF feedback electronics, we have successfully demonstrated a novel and economic long-term stabilization scheme for a 10 GHz 0.8 ps asynchronously mode-locked Er-fiber soliton laser by controlling the cavity length to lock the deviation frequency at 25 kHz. The results achieved in Chapter 3 and Chapter 4 show that the high-repetition-rate, femtosecond ASM Er-fiber laser should be able to be used in practical applications.

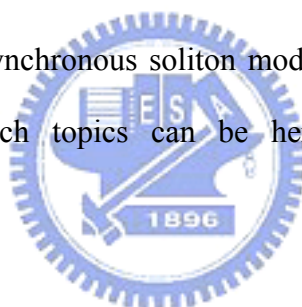
Section 2-5 and Chapter 5 describe the experimental observations of soliton bound states. Typical soliton bound states observed in passively mode-locked fiber laser, including short-range soliton interaction and long-range soliton interaction, are shown in Section 2-5. In addition, new stable bound soliton pairs occurring in a 10 GHz hybrid FM Er-fiber mode-locked laser are presented in Chapter 5. 1177 soliton pairs are created to simultaneously circulate in the laser cavity. The two solitons in the soliton pair have the identical pulse shape and are with the anti-phase (π phase difference). Their time separation is about three times the FWHM soliton-width and varies with the phase modulation strength. These closely adjacent soliton pairs are stably formed through the balance between the soliton direct interaction and the

effective attracting force introduced by the phase modulation and the negative GVD of the cavity.

All the investigation and results demonstrated in this thesis show the versatility of mode-locked fiber soliton lasers. They can be the reliable ultrashort pulse laser sources at high repetition rates for many practical applications as well as feasible platforms for exploring new interesting soliton phenomena.

6.2 Future Work

In this thesis, we have successfully developed new methods to implement high-repetition-rate, femtosecond Er-fiber lasers in the 1.55 μm band, especially based on the technique of asynchronous soliton mode-locking. From these achieved results, some related research topics can be here given for possible further investigation.



(1) 40 GHz asynchronously mode-locked (ASM) Er-fiber soliton laser

The methods of asynchronous soliton mode-locking used in Chapter 3 and the long-term stabilization scheme developed in Chapter 4 can be further utilized to demonstrate the ASM Er-fiber soliton laser at 40 GHz repetition rate for next-generation high-speed optical fiber communication systems. Up to now, we have already achieved some experimental results of 20 and 30 GHz ASM Er-fiber soliton lasers, and all these results show the feasibility to demonstrate the repetition rate up to 40 GHz if the cavity dispersion is well controlled and the pump power is larger enough. Moreover, the ASM Er-fiber soliton laser also shows the tendency to generate shorter pulse when the repetition rate is increased from 10 GHz to higher repetition

rate. The shortest pulse width observed in our 30 GHz ASM Er-fiber soliton lasers has been found to be nearly 600 fs.

(2) 1 μ m Yb-fiber mode-locked lasers

Recently, a lot of research works have been focused on the development of 1 μ m mode-locked Yb-fiber lasers, since 1 μ m femtosecond pulsed source are useful in many applications, such as multiphoton microscopy [1], supercontinuum generation for optical coherent tomography (OCT) [2], and high-repetition-rate femtosecond combs for precise frequency metrology [3]. Our results achieved in the 1.55 μ m femtosecond Er-fiber lasers should also can be well applied to 1 μ m femtosecond Yb-fiber lasers. However, for silica-based fibers, group velocity dispersion (GVD) is normal when the wavelength range below 1300 nm, which means that the cavity dispersion compensation/control is required for Yb-fiber lasers working in the soliton regime. The methods to solve this problem include using bulk diffraction gratings or prisms [4], hollow-core photonic bandgap (PBG) fiber [5], solid-core PBG fiber [6], or two-mode silica fiber with mode coveter of long period fiber grating (LPG) [7].

(3) Femtosecond pulse amplification

With the rapid progress in the technology of fiber fabrication and design, such as double-cladding or large-mode-area gain fibers, high-power Yb doped or Er/Yb codoped fiber amplifiers can be used to amplify femtosecond mode-locked fiber lasers. However, the distortion of pulse shape or pulse breaking during femtosecond pulse amplification due to Kerr nonlinearity are the issues need to be considered [8]. The pulse shape distortion and pulse breaking can be eliminated by employing the

configuration of chirped-pulse amplification (CPA) [9,10]. Recently, the parabolic pulse amplifier combined with a pulse compressor has been shown to be able to provide an efficient method to amplify and compress femtosecond pulse [11,12]. Therefore it is possible to boost the pulse energy of mode-locked fiber lasers from n J to μ J (even mJ) through the use of fiber power amplifiers [13-15]. High energetic femtosecond pulses can be further used in nonlinear frequency conversion [16], supercontinuum generation for precise measurements [3,17], or waveguide fabrication by direct writing[18]. These and other applications should also be worthwhile for possible future investigation.



References for Chapter 6:

- [1] T.-H. Tsai, S.-P. Tai, W.-J. Lee, H.-Y. Huang, Y.-H. Liao, and C.-K. Sun, "Optical signal degradation study in fixed human skin using confocal microscopy and higher-harmonic optical microscopy," *Opt. Express* **14**, 749 (2006).
- [2] H. Lim, Y. Jiang, Y. Wang, Y.-C. Huang, Z. Chen, and F. W. Wise, "Ultrahigh-resolution optical coherence tomography with a fiber laser source at 1 μm ," *Opt. Lett.* **30**, 1171 (2003).
- [3] T. Udem, R. Holzwarth, and T. W. Hänsch, "Optical frequency metrology," *Nature* **416**, 233 (2002).
- [4] F. Ö. Ilday, J. R. Buckley, H. Lim, F. W. Wise, and W. G. Clark, "Generation of 50-fs, 5-nJ pulse at 1.03 μm from a wave-breaking-free fiber laser," *Opt. Lett.* **28**, 1365 (2003).
- [5] H. Lim and F. W. Wise, "Control of dispersion in a femtosecond ytterbium laser by use of hollow-core photonic bandgap fiber," *Opt. Express* **12**, 2231 (2004).
- [6] A. Isomäki and O. G. Okhotnikov, "All-fiber ytterbium soliton mode-locked laser with dispersion control by solid-core photonic bandgap fiber," *Opt. Express* **14**, 4368 (2006).
- [7] S. Ramachandran, S. Ghalmi, J. W. Nicholson, M. F. Yan, P. Wisk, E. Monberg, and F. V. Dimarcello, "Demonstration of Anomalous Dispersion in a Solid, Silica-Based Fiber at $\lambda < 1300\text{ nm}$," Conference on Optical Fiber Communication (OFC'2006), Paper PDP, Anaheim, CA, Mar. 2006 (Optical Society of America, Washington, DC, 2006).
- [8] S. Zhou, L. Kuznetsova, A. Chong, and F. W. Wise, "Compensation of nonlinear phaseshifts with third-order dispersion in short-pulse fiber amplifiers," *Opt. Express* **13**, 4869 (2005).

- [9] D. Strickland and G. Mourou, "Compression of amplified chirp optical pulses," *Opt. Commun.* **56**, 219 (1985).
- [10] S. Kane and J. Squier, "Grating compensation of third-order material dispersion in the normal dispersion regime: Sub-100-fs chirped-pulse amplification using a fiber stretcher and grating-pair compressor," *IEEE J. Quantum Electron.* **31**, 2052 (1995).
- [11] V. I. Kruglov, A. C. Peacock, J. M. Dudley, and J. D. Harvey, "Self-similar propagation of high-power parabolic pulses in optical fiber amplifiers," *Opt. Lett.* **25**, 1753 (2000).
- [12] D. B. Soh, J. Nilsson, and A. B. Grudinin, "Efficient femtosecond pulse generation using a parabolic amplifier combined with a pulse compressor. II. Finite gain-bandwidth effect," *J. Opt. Soc. Am. B* **23**, 10 (2006).
- [13] T. Schreiber, C. K. Nielsen, B. Ortac, J. Limpert, and A. Tünnermann, "Microloule-level all-polarization-maintaining femtosecond fiber source," *Opt. Lett.* **31**, 574 (2006).
- [14] F. Röser, J. Rothhard, B. Ortac, A. Liem, O. Schmidt, T. Schreiber, J. Limpert, and A. T. A. Tünnermann, "131 W 220 fs fiber laser system," *Opt. Lett.* **30**, 2754 (2005).
- [15] A. Shirakawa, J. Ota, M. Musha, K. Nakagawa, K. Ueda, Jacob R. Folkenberg, and J. Broeng, "Large-mode-area erbium-ytterbium-doped photonic-crystal fiber amplifier for high-energy femtosecond pulses at 1.55 μm ," *Opt. Express*, **13**, 1221 (2005).
- [16] K. Moutzouris, F. Sotier, F. Adler, A. Leitenstorfer, "Highly efficient second, third and forth harmonic generation from a two-branch femtosecond erbium fiber source," *Opt. Express* **14**, 1905 (2004).
- [17] J. Zhang, Z. H. Lu, and L. J. Wang, "Precision measurement of the refractive

index of air with frequency combs,” Opt. Lett. **30**, 3314 (2005).

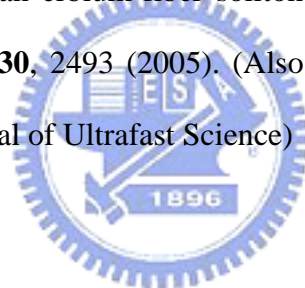
- [18] R. R. Thomson, S. Campbell, I. J. Blewett, A. K. Kar, and D. T. Reid, “Optical waveguide fabrication in z -cut lithium niobate (LiNbO_3) using femtosecond pulses in the low repetition rate regime,” Appl. Phys. Lett. **88**,111109 (2006).



List of Publications

[Journal]

1. W.-W. Hsiang, C.-Y. Lin, and Y. Lai, "Stable new bound soliton in a 10 GHz hybrid frequency modulation mode-locked Er-fiber laser," *Opt. Lett.* **31**, 1627 (2006).
2. W.-W. Hsiang, C.-Y. Lin, N. K. Sooi, and Y. Lai, "Long-term stabilization of a 10 GHz 0.8 ps asynchronously mode-locked Er-fiber soliton laser by deviation-frequency locking," *Opt. Express* **14**, 1882 (2006). (Also selected for the May, 2006 issue of the Virtual Journal of Ultrafast Science)
3. W.-W. Hsiang, C.-Y. Lin, M.-F. Tien, and Y. Lai, "Direct generation of 10 GHz 816 fs pulse train from an erbium-fiber soliton laser with asynchronous phase modulation," *Opt. Lett.* **30**, 2493 (2005). (Also selected for the October, 2005 issue of the Virtual Journal of Ultrafast Science)



[International Conference]

1. W.-W. Hsiang, C.-Y. Lin, and Y. Lai, "Observation of stable bound soliton pairs in a 10 GHz actively FM mode-locked Er-fiber laser," Conference on Lasers and Electro-Optics (CLEO 2006), Paper JWB58, Long Beach, CA, May 2006 (Optical Society of America, Washington, DC, 2006).
2. W.-W. Hsiang, C.-Y. Lin, N. K. Sooi, and Y. Lai, "Stabilizing a 10 GHz 0.8 ps Asynchronously Mode-Locked Er-Fiber Soliton Laser by Deviation-Frequency Locking," Conference on Optical Fiber Communication (OFC 2006), Paper OThC7, Anaheim, CA, Mar. 2006 (Optical Society of America, Washington, DC, 2006).
3. C.-Y. Lin, W.-W. Hsiang, M.-F. Tien and Y. Lai, "Direct generation of 10GHz

816fs pulse train from an asynchronous modelocked Er-fiber laser”, Conference on Lasers and Electro-Optics (CLEO 2005), Paper CTuCC5, Baltimore, MD, May 2005 (Optical Society of America, Washington, DC, 2005).

4. W.-W. Hsiang, C.-C. Chung and Y. Lai, “Observation of Pulse Repetition Rate Multiplication in a Stretched-Pulse Additive-Pulse-Modelocking Er-Fiber Laser”, Paper TU3G (6)-4, CLEO/Pacific-Rim 2003, Taipei, Taiwan.
5. M. Tien, W.-W. Hsiang, and Y. Lai, “A femtosecond hybrid mode-locked Er-fiber soliton laser by asynchronous phase modulation”, Paper TU3G (6)-3, CLEO/Pacific-Rim 2003, Taipei, Taiwan.
6. W.-W. Hsiang, C.-H. Lim, G.-C. Liang, A. H. Kung, A. Schmohl, A. Miklos, and P. Hess, “Photoacoustic trace gas detection using pulsed grazing-incidence PPLN optical parametric oscillator”, Paper MF2-3, CLEO/Pacific Rim 2001, Chiba, Japan.



[Domestic Conference]

1. W.-W. Hsiang, C.-Y. Lin, N. K. Sooi, and Y. Lai, “Long-term stabilization of a 10 GHz 0.8 ps asynchronously hybrid mode-locked Er-fiber soliton laser”, C-FR-V1-3, Optics and Photonics Taiwan 2005.
2. K.-C. Hsu, L.-G. Sheu, W.-W. Hsiang, and Y. Lai, “Nonlinear photosensitive effect on in refractive index profile and spectral response of fiber Bragg grating”, B-SA-III 9-4, Optics and Photonics Taiwan 2005.
3. C.-L. Lee, W.-W. Hsiang, and Y. Lai, “ Design of optimal second-order nonlinear QPM fiber grating for second-harmonic generation with pulse shaping”, PB-SU1-04, Optics and Photonics Taiwan 2004.
4. C.-Y. Lin, W.-W. Hsiang, M.-F. Tien and Y. Lai, “A 10 GHz femtosecond hybrid mode-locked Er-fiber soliton laser by asynchronous phase modulation”,

C-SA-IV 2-7, Optics and Photonics Taiwan 2004.

[Patents/Invention Disclosure]

1. W.-W. Hsiang, C.-Y. Lin, N. K. Sooi, and Y. Lai, “Method and Apparatus for Stabilizing Asynchronously Mode-Locked Lasers”, TW patent applying.

